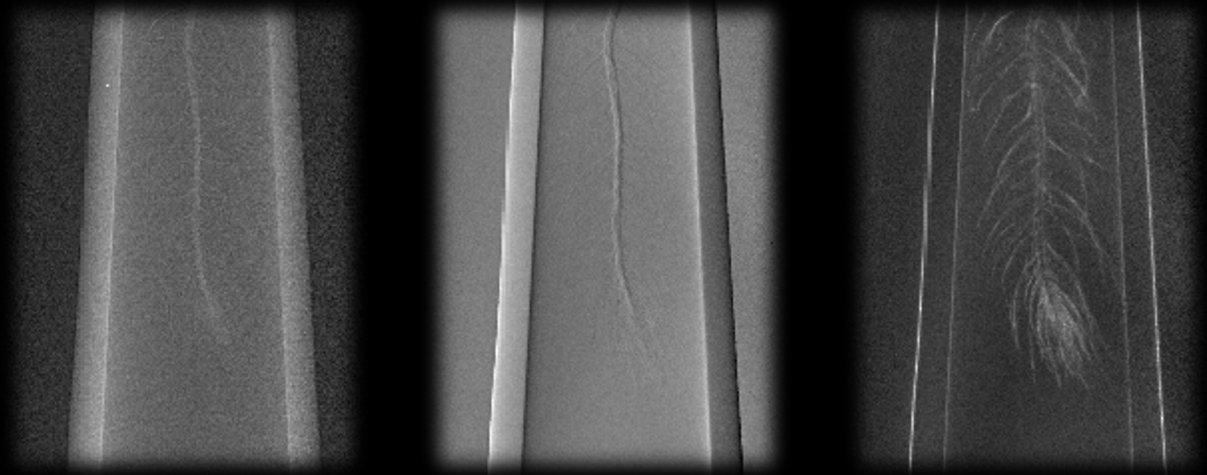


# Bachelor Thesis

Institute for Biomedical Engineering, ETH Zurich



# System Optimization and Software Design in Grating- Interferometry X-Ray Imaging Laboratories

Lionel Peer

Supervision: Prof. Dr. Marco Stampanoni  
Advisor: Dr. Maxim Polikarpov



## ABSTRACT

The X-Ray Tomography Group of the Biomedical Engineering Institute at ETH Zurich operates an X-ray grating interferometer located at the Paul Scherrer Institut. This setup is extensively used for laboratory X-ray imaging of samples for materials sciences as well as biological and medical ones. As part of ongoing research activities at this setup, I was granted the responsibility to design high-level operation and data processing software in the context of my Bachelor's thesis. Before my arrival the setup had been operated with low-level software and in order to allow for hardware independent operation and reduce acquisition times, a high level software package was created. The written operation software allows for a quick change of hardware components and more can be easily added. In the case of one detector, a significant reduction in overhead time was achieved. The high-level approach ensures the safe operation by group members with very little experience, making it available as a research tool for larger parts of the group. Further, a collection of frequently used data processing functions was created and their capabilities extended, such that they can handle different types of inputs. Tomographic reconstruction had so far only been done using parallel geometries. This functionality was extended such that it now considers the cone shaped geometry of the real system and makes use of the highly parallelizable architecture of GPUs, while operational simplicity for the user was kept at the same level.



# ACKNOWLEDGMENTS

My time at TOMCAT was an intense and very interesting one. I got to first hand experience day-to-day laboratory operations and was included in every single process. I would like to thank Prof. Dr. Marco Stampanoni, my supervisor and the group leader of TOMCAT, for making my first research experience possible and introducing me to the world of X-ray imaging.

A special thanks goes to Dr. Maxim Polikarpov who was my direct advisor during these 14 weeks. He gave me a lot of liberty with my research and I was always welcome to introduce new ideas. This gave me the chance to get a broad view of not only grating interferometry but X-ray imaging and computed tomography as a whole.

Further I would like to thank Dr. Michał Rawlik, the leader of our neighboring group that focuses on breast CT, and Simon Spindler, who both gave me great advice on simulations and tomographic reconstruction. I was always welcome to ask questions, be it during the lunch breaks or via email.

Another opportunity that I was given over the course of this thesis, was the chance to test the performance of newly produced high aspect ratio absorption gratings. For this I would like to thank Dr. Lucia Romano, Zhitian Shi and Dr. Konstantins Jefimovs with whom I got to spend a great time in the lab.

Finally I would like to thank Lars Lenherr, who wrote his Bachelor's thesis during the same time in Michał's group, for the scientific exchange that we had, both about the setups and the Bachelor's thesis as such.



# CONTENTS

|  | Seite |
|--|-------|
| 1. Introduction  | 1     |
| 2. Theory  | 3     |
| 2.1. X-Rays and Matter . . . . .                                       | 3     |
| 2.2. Talbot Effect . . . . .   | 4     |
| 2.3. Fractional Talbot Effect & Moiré Patterns . . . . .               | 6     |
| 2.4. Talbot-Lau Interferometer . . . . .                               | 7     |
| 2.5. Image Acquisition, Phase Retrieval & Quality Assessment . . . . . | 8     |
| 2.5.1. Visibility . . . . .  | 8     |
| 2.5.2. Angular Sensitivity . . . . .                                   | 9     |
| 2.6. Computerized Tomography & Tomographic Reconstruction . . . . .    | 9     |
| 2.6.1. Mathematical Basis . . . . .                                    | 10    |
| 2.6.2. Reconstruction Algorithms . . . . .                             | 10    |
| 3. Lab Setup   | 15    |
| 3.1. Detector . . . . .  | 15    |
| 3.2. Gratings . . . . .  | 16    |
| 3.3. Motorized Towers . . . . .  | 17    |
| 3.4. X-Ray Source . . . . .  | 17    |
| 3.5. Placing and Alignment of Components . . . . .                     | 18    |
| 4. Operation Software  | 21    |
| 4.1. Detector Operation . . . . .                                      | 21    |
| 4.1.1. Acquiring Images with Eiger . . . . .                           | 23    |
| 4.1.2. Speeding up the Tomographic Process . . . . .                   | 23    |
| 4.2. Motor Operation . . . . .   | 24    |
| 4.3. The Lab CT as one Object . . . . .                                | 25    |
| 4.4. Conclusions & Perspective . . . . .                               | 26    |

|  |           |
|--|-----------|
| <b>5. Data Processing</b>  | <b>29</b> |
| 5.1. Reading Detector Output . . . . .   | 29        |
| 5.2. Measuring Visibility & Angular Sensitivity . . . . .                                      | 30        |
| 5.3. Extracting the 3 Images . . . . .   | 31        |
| 5.4. Tomographic Reconstruction . . . . .  | 34        |
| 5.4.1. The Reconstruction Class . . . . .  | 34        |
| 5.4.2. Phantom Creation & Performance Testing . . . . .  | 36        |
| 5.5. Conclusions & Perspective . . . . .   | 38        |
| <b>6. Conclusions &amp; Perspective</b>  | <b>39</b> |
| <b>A. Testing of Bottom-Up Gold Filled High Aspect Ratio Gratings for X-Ray Interferometry</b> | <b>41</b> |
| A.1. Grating Tests . . . . .   | 41        |
| A.2. Conclusion . . . . .  | 43        |
| <b>B. Operation &amp; Reconstruction Software</b>  | <b>47</b> |
| B.1. Requirements for operating the setup . . . . .  | 47        |
| B.2. Requirements for operating the reconstruction . . . . .                                   | 47        |
| B.3. Operation Software . . . . .  | 48        |
| B.4. Data Processing Software . . . . .  | 64        |
| <b>References</b>  | <b>75</b> |
| <b>Image Sources</b>   | <b>79</b> |

# 1 INTRODUCTION

X-ray imaging started with the detection of X-rays by W. Röntgen and the subsequent publication of the first X-ray image in 1895. Soon, single projections were not enough anymore and driven by the motivation to get an insight into the rib cage, without the ribs interfering, axial tomography was invented in the late 1930s and 40s. Those axial tomographs were purely mechanical and only in the 1960s, with the rise of the digital technology, the idea of a computer-based back projection arose. This led to the creation of CT by A. Cormack and G. Hounsfield, for which they were awarded the Nobel prize in 1979. In parallel, phase contrast imaging was developed for the visible light spectrum and is a well established technology for microscopy [5]. Adaptation using X-ray was slow due to challenges in the microfabrication process of X-ray optical elements. Nevertheless, interferometry for synchrotrons was explored and successfully deployed during the 1990s [15] and early 2000s. Subsequently, in 2006, the development of a Talbot-Lau interferometer setup with a conventional X-ray tube was first published [11]. This opened the doors for future medical applications since the better contrast in soft tissues has great potential, for example in the detection of breast cancer.

Such a system, has been installed at the X-ray tomography group of Prof. Dr. M. Stampanoni at the Paul Scherrer Institut. It offers high spatial resolution ( $10\ \mu\text{m}$ ) in a field of view of 5-15 cm. So far, typical acquisition times for tomographic scans ranged from 15 hours to 3 days, depending on the setup geometry and the number of projections. The motivation behind this thesis was to bring the acquisition times down by streamlining the process, make it universal for different hardware components and provide a software infrastructure for quick reconstruction of the acquired projections. Eventually this setup should be able to acquire and process high resolution phase contrast tomography, for example of histopathological samples, in a time frame of 2-3 h. The high-level approach that the software should follow would also allow this setup to be used as a research tool for other members of the group. After getting comfortable with the operation of the single components, points of optimization can be identified with which this high-level framework should be designed. By optimizing the interaction between the hardware components, acquisition times should be brought down. Tomographic reconstruction should be enhanced by introducing a simplified access to powerful GPU optimized reconstruction

algorithms. Those algorithms are not only faster, but they also take the diverging X-ray beam into account, therefore closer resembling the real setup.

The first part of the thesis will cover the theory behind phase contrast X-ray imaging using interferometers and the reconstruction of acquired tomographic data sets. The second part covers the different hardware components and improvements made in this respect. Further, the last two parts, will present the software packages for controlling the setup and for the reconstruction. The emphasis will lie on improvements that simplify and speed up operation as well as the processing of data.

# 2 THEORY

The goal of this chapter is to lay out the mathematical and physical foundation behind X-ray interferometry used for phase contrast imaging and tomographic acquisition and reconstruction. Understanding this is of importance when looking at the operation and reconstruction software packages and for the discussion of experimental results.

## 2.1. X-Rays and Matter

X-rays are photons with an Energy of  $E = \frac{hc}{\lambda}$ , where  $h$  is Planck's constant, which is experimentally derived, and  $\lambda$  is the wavelength of the corresponding photon. While visible light has wavelengths of 400 nm (violet) to 700 nm (red), the energy range of diagnostic X-rays, which is the primary focus of this thesis, lies in between 10 keV and 150 keV and therefore the wavelengths are significantly smaller (0.12 nm to 0.008 nm). The dominating effects of matter interaction at this energy range are photoelectric absorption, Compton scattering & Rayleigh scattering. Photoelectric absorption is a contributor to the attenuation or decrease in intensity of the incoming X-ray beam, Compton scattering both attenuates and scatters, while Rayleigh only leads to scattering of the photons [19, p. 8]. X-rays follow the wave-particle duality and interferometric imaging makes use of their wave nature with the help of diffraction and refraction.

In order to understand the X-ray and matter interaction it is helpful to start with plane waves propagating in a medium, mathematically described by the following equation:

$$E(r, t) = \text{Re}\{\underline{E}(r)e^{-i\omega t}\} \quad (2.1)$$

$\underline{E}$  is the complex field amplitude of the real time dependent field  $E$  and  $\underline{E}$  is again described with the help of field vector  $\underline{E}_0$  and wave vector  $r$ , determining polarization and propagation directions.

$$\underline{E}(r) = \underline{E}_0 e^{\pm ik \cdot r} \quad (2.2)$$

Without loss of generality, but for reasons of simplicity, it is helpful to constrain calculations to plane waves travelling in z-direction, incident to an object in space. The underscore of the vectorial field quantities will be dropped from now on and  $k_z = 2\pi/\lambda$  simplifies to a scalar quantity, the wave number.

$$E_{in}(z) = E_0 e^{ik_z z} \quad (2.3)$$

As described by [19, p. 11], the total interaction of such an X-ray wave travelling through a sample between  $z = 0$  and  $z = z_0$  can be described by a line integral along the z-axis that sums all interaction. This results in the following relation between incoming and outgoing waves.

$$E_{out} = E_{in} e^{ik \int_0^{z_0} n(z) dz} \quad (2.4)$$

$n(z)$  is the spatial distribution of the complex coefficient of refraction  $n = 1 - \delta + i\beta$ , where  $\beta$  is related to the attenuation properties of the material and  $\delta$  to the phase shifting properties. Putting this into Eq. 2.4 yields a term consisting of a propagative part, a phase shifting part and an attenuation part.

$$E_{out} = E_{in} e^{ikz_0} e^{-ik \int_0^{z_0} \delta(z) dz} e^{-k \int_0^{z_0} \beta(z) dz} \quad (2.5)$$

Deriving attenuation  $A$  (influence on the amplitude) and phase difference from Eq. 2.5, the resulting equations are the following [19, p. 11]:

$$A = 1 - \left( \frac{|E_{out}|}{|E_{in} e^{ikz_0}|} \right)^2 \quad (2.6a)$$

$$\phi = \arg(E_{out}) - \arg(E_{in} e^{ikz_0}) \quad (2.6b)$$

As can be seen from the equations, the incoming field ( $E_{in}$ ) that propagated through the sample space without the sample present ( $E_{in} e^{ikz_0}$ ), must be measured as well. From now on, this will be the so called *flat-field* image. X-ray detectors use different technologies to measure the intensity of the beam, therefore determining  $A$  from Eq. 2.6a is straightforward. Accessing the information hidden in the phase of the outgoing wave is more complicated, and its process will be explained in detail in the next sections.

## 2.2. Talbot Effect

In 1836, Henry Fox Talbot made the observation that light, incident to a grating, will reproduce the exact structure of the grating, if a screen is placed at certain distances behind the grating.

In 1881 Lord Rayleigh was the first to quantify these distances as:

$$z = m \cdot \frac{d^2}{\lambda} \quad (2.7)$$

For these distances,  $d$  is the period of the grating,  $\lambda$  the wavelength of the incident particle and  $m$  is an arbitrary integer value. The actual reproduction happens at double these distances,  $z_T = m \cdot 2d^2/\lambda$ , the image at  $d^2/\lambda$  is shifted to the side by half the grating period [12, p. 196]. The value of  $z_T$  will from now on be called *Talbot distance* and the integer  $m$  will be called the *Talbot order*.

In order to calculate this value, one can imagine a wave incident to the grating in the  $(x, y)$  plane at  $z = 0$ . The grating structure can be imagined as vertical, which corresponds to parallel to the y-axis. The incident wave has an angle of incidence of  $\theta$  between propagation direction and the  $(y, z)$  plane. This angle is of interest since the grating acts on the wave component perpendicular to both the grating structure and the propagation direction, which is the x-axis. As presented by [2] the field behind the grating can be calculated by starting with the projection of the wave vector onto the  $x$  axis  $k_x = k \sin(\theta)$ , yielding the wave of interest as  $\psi = e^{ik_x x}$  and calculating the wave directly behind the grating as follows:

$$\psi(x, +0) = \psi(x, -0)T(x) = \sum_n A_n e^{i(k_x + 2\frac{\pi}{d}n)x} \quad (2.8)$$

In this equation,  $T(x) = \sum_n A_n e^{i2\frac{\pi}{d}nx}$  is the grating transfer function. It can be observed that the grating adds multiples of  $2\pi/d$  to the wave vector  $k_x$ , which means that everything so far is perpendicular to the optical axis. The other wave vector component,  $k_z$ , can be derived from the total wave vector and the above x-direction component:

$$k_z = \sqrt{k^2 - \left(k_x + 2\frac{\pi}{d}n\right)^2} \quad (2.9)$$

Using paraxial- and Taylor approximations, as shown by [20], this can be simplified to:

$$k_z \approx k - \frac{(k_x + 2\frac{\pi}{d}n)^2}{2k} \quad (2.10)$$

Adding this to the calculation from above, the complete field behind the grating presents itself as the following:

$$\psi(x, z) = \sum_n A_n e^{i(k \sin(\theta) + 2\frac{\pi}{d}n)x + i\left(k - \frac{(k \sin(\theta) + 2\frac{\pi}{d}n)^2}{2k}\right)z} \quad (2.11)$$

For the *Talbot effect* to happen, spatially coherent waves are required to be incident to the grating, therefore  $\sin(\theta) = 0$ . Also putting in the relation that  $k = 2\pi/\lambda$  the field simplifies to:

$$\psi(x, z) = \sum_n A_n e^{i2\frac{\pi}{d}nx} e^{i2\frac{\pi}{\lambda}z} e^{-in^2\frac{\pi\lambda}{d^2}z} \quad (2.12)$$

The second term is not of interest, since it is independent of  $n$  and introduces a global phase. It is visible that  $e^{-in^2\frac{\pi\lambda}{d^2}z}$  becomes  $e^{-i2m\pi\cdot n^2}$  for  $z = m \cdot 2d^2/\lambda$ , which was the before defined Talbot distance. Since this term's exponent includes an integer multiple of  $2\pi$ , it is always one at those distances. The following field at Talbot distances is formed, corresponding exactly to the transfer function of the grating:

$$\psi(x, z = m \cdot 2d^2/\lambda) = \sum_n A_n e^{i2\frac{\pi}{d}nx} \quad (2.13)$$

### 2.3. Fractional Talbot Effect & Moiré Patterns

When using phase gratings, a similar effect can be observed, called *Lohmann images* by Suleski in [16], instead of *Talbot self images*. They appear at fractions of the Talbot distance and are therefore part of a class called *Fractional Talbot Effects*. The main motivation behind using phase gratings instead of absorption gratings is, that they can be manufactured from poorly absorbing material, offering very high efficiency compared to standard gratings, where absorption is necessary for their function. Suleski lists 36 different combinations of duty cycles and phase shift values producing such images, this thesis will only look at  $\pi$  and  $\pi/2$  shifting gratings. For a specific wave length, from now on called design energy, and a phase grating that causes a phase shift of  $\phi = \pi/2$  at this energy and has duty cycle 50%, this distance is 1/4th of the original Talbot distance or:

$$z_{par,\pi/2} = m \cdot \frac{p_1^2}{2\lambda} \quad (2.14)$$

For a phase shift of  $\pi$ , such an image forms at 1/16th of the Talbot distance, but here the period of the Lohmann image is half the grating period, as also stated by [3].

$$z_{par,\pi} = m \cdot \frac{p_1^2}{8\lambda} \quad (2.15)$$

With the help of geometric magnification, this was the grating specification used in the setup during the course of this thesis. With  $s$  being the complete setup length and  $l$  the distance between the phase grating and a micro focus source, the periods get magnified by  $M = \frac{s}{l}$ .

For this reason, the distances were deliberately indexed *par*, because they are only true for

a parallel shaped geometry. For a cone shaped incident beam, those maxima of intensity are reached at the following distances, as stated by [4], where  $l$  is again the source-phase grating distance:

$$z_{cone} = \frac{l}{l - z_{par}} z_{par} \quad (2.16)$$

Since the goal is to detect changes when a sample is placed in the beam, analyzing shifts in this pattern due to a refractive change is necessary. Unfortunately the pixel size of the detector is significantly bigger than the period of the pattern which makes a direct analysis impossible. In order to tackle this problem, an analyzer grating instead of the detector itself, is placed at such a fractional Talbot distance behind the phase grating. The pattern formed by the phase grating should have the same periodicity as the analyzer and overlap with its structure. A refractive change in the beam will then immediately translate into an intensity change on the detector which follows directly behind this analyzer grating.

## 2.4. Talbot-Lau Interferometer

In order to reach the needed coherence, a source grating is used that creates individually coherent line sources. Sufficient coherence is a premise for the use of a grating like the one from section 2.2 or 2.3. From now on this source grating will be called  $G_0$ , the phase grating  $G_1$  and the analyzer grating  $G_2$ . For these gratings, the periods need to have the following geometry, where  $l$  is now the length between  $G_0$  and  $G_1$  and  $d$  is the distance between  $G_1$  and  $G_2$  corresponding to the fractional Talbot distance [11]:

$$p_{G_0} = \frac{l}{d} p_{G_2} \quad (2.17)$$

This is called a *Talbot-Lau configuration* and by placing the gratings according to above equation, the incoherence between the single sources works constructively. [22].

The symmetric setup with  $\pi$ -shifting  $G_1$  and the same periods everywhere emerges as one possible configuration for such a Talbot-Lau interferometer. Condition 2.17 is fulfilled and the magnification factor of  $M = 2$  increases the period of the Lohmann image at  $z_{par,\pi}$  to match the period of  $G_2$ . An example of such a symmetric setup with gratings of period  $2\mu\text{m}$  and  $\pi$ -shifting  $G_1$  is shown in Fig. 2.1.

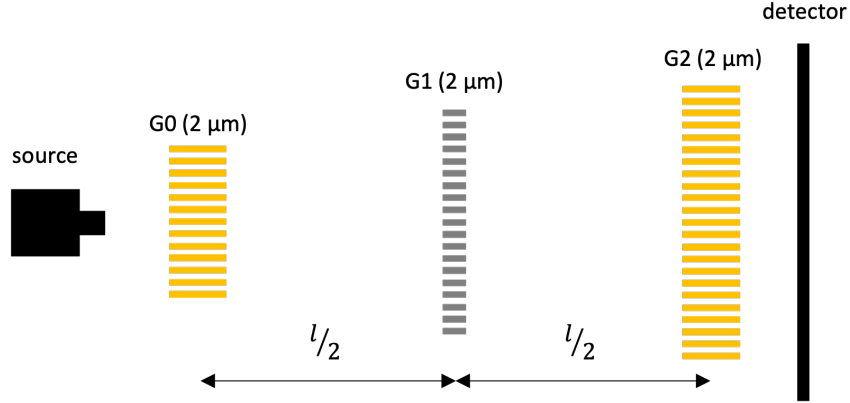


**Fig. 2.1.:** Symmetric setup with gold filled absorption gratings and  $\pi$  shifting phase grating. Sample placement is between  $G_0$  and  $G_1$

## 2.5. Image Acquisition, Phase Retrieval & Quality Assessment

Data acquisition is done using a phase stepping technique. The analyzer grating is moved in  $x$ -direction, the direction of the grating modulation, over the course of one grating period and an image is taken at every step.

The phase stepping leads to a phase stepping curve in each pixel, from which absorption contrast ( $amp$ ), differential phase contrast ( $dpc$ ) and scattering or dark-field contrast ( $dci$ ) signals can be derived, using Fourier analysis. The values  $a_{0,1}$  and  $\phi_1$  in the formulas below correspond to norm and phase of the first and second Fourier coefficients for either the flat-field phase stepping curve ( $ref$ ) or the phase stepping curve with the sample ( $sam$ ). The formula for absorption contrast corresponds to the formula mentioned in Eq. 2.6a. For phase information, the second Fourier coefficient is used (unlike Eq. 2.6b), therefore it is called the *differential* phase contrast image [19, p. 21].

$$amp = 1 - \frac{a_{0,sam}}{a_{0,ref}} \quad (2.18a)$$

$$dpc = \phi_{1,sam} - \phi_{1,ref} \quad (2.18b)$$

$$dci = \frac{a_{1,sam}}{a_{0,sam}} \cdot \frac{a_{0,ref}}{a_{1,ref}} \quad (2.18c)$$

### 2.5.1. Visibility

Since such an interferometer works with polychromatic sources and not everything gets absorbed in the gold inlays of the absorption gratings, the visibility of the fringes is an important

metric to determine its performance.

As demonstrated by [17], the phase stepping curve  $I_p(x)$  is a convolution of the optimal interference pattern for coherent sources  $I_c(x)$ , the source intensity profile at the detector  $S'(x)$ , and the transmission of the analyzer grating  $G_2$  ( $G(x)$ ). Because of the transmission function,  $I_p(x)$  is periodic in the  $G_2$  grating period and the visibility can be calculated using Fourier analysis:

$$V = \frac{I_{p,max}(x) - I_{p,min}(x)}{I_{p,max}(x) + I_{p,min}(x)} = 2 \frac{a_1}{a_0} \quad (2.19)$$

Here,  $a_{0,1}$  are again the respective Fourier coefficients derived from the phase stepping curve. It is worth noting that assuming G0 and G2 as perfectly absorbing gratings with duty cycle 50%, the visibility would reach 51.6% [17].

### 2.5.2. Angular Sensitivity

A different metric for measuring the performance of a grating interferometry is the smallest detectable refraction angle. It is dependent on the inter grating distance of  $G_1$  and  $G_2$  ( $d$ ), the standard deviation ( $\sigma_\phi$ ) of the differential phase contrast image  $dpc = \phi_{1,sam} - \phi_{1,ref}$  and the  $G_2$  period, as presented by [18].

$$\alpha_{min} = \frac{p_2}{2\pi d} \frac{l}{l_s} \sigma_\phi \quad (2.20)$$

The distances  $l$  and  $l_s$  are the distances  $G_0$ - $G_1$  and  $G_0$ -sample respectively. Since  $l_s$  is in any case the smaller distance than  $l$ , the sample should be placed as close as possible to  $G_1$  in order to minimize  $\alpha_{min}$ . Longer propagation distances ( $d$ ) and smaller grating periods are also beneficial in this regard.

## 2.6. Computerized Tomography & Tomographic Reconstruction

Computerized tomography has revolutionized diagnostic radiology and the 1979 Nobel prize in physiology and medicine was awarded for its development. Many others in the field have followed, for example the 2003 Nobel prize for advancements in magnetic resonance imaging, a related method that also uses the reconstruction from projections [6].

The idea behind such imaging methods is that, given a sufficient amount of information from different angular projections through the object, the cross section of the object can be reconstructed.

### 2.6.1. Mathematical Basis

Even though reconstruction can be done for any kind of projection image mentioned in 2.5, this section will show it using absorption projections. The formulas hold true for the other images as well.

Assuming an infinitely small slice of the object between  $z = 0$  and  $z = D$ , the attenuation along a line passing through this slice can be described as:

$$m = \int_0^D \mu(x, y) dz \quad (2.21)$$

The value  $\mu$  is the attenuation coefficient, closely related to  $\beta$  from the complex coefficient of refraction mentioned in 2.1 by  $\mu = 2k\beta$ , with  $k$  being the wave number. The goal is to derive the spatial distribution of  $\mu(x, y)$  in the whole slice from this information.

The mathematical basis for this reconstruction had already been provided by Johann Radon in 1917 [6, p. 35].

$$\mu_\epsilon(x, y) = -\frac{1}{2\pi^2} \lim_{\epsilon \rightarrow 0} \int_\epsilon^\infty \frac{1}{q} \int_0^{2\pi} m_1(x \cos \theta + y \sin \theta + q, \theta) d\theta dq \quad (2.22)$$

In this formula,  $m_1$  is the partial derivative of the the line integral  $m(l = x \cos \theta + y \sin \theta + q, \theta)$  with respect to  $l$ . Looking from above onto the slice like in Fig. 2.2,  $l$  is the deviation to the side from the center of rotation and  $\theta$  is the angle at which the line integral is taken. The analogy in a real setup is the following: a slice represents a pixel row on the detector,  $l$  one of these pixels and all  $l$  with a certain  $\theta$  form one projection of the slice. Even though the formula is complicated, it is visible that, given infinitely small  $l$  and  $\theta$ , the attenuation coefficient distribution in the slice could be completely and uniquely reconstructed.

### 2.6.2. Reconstruction Algorithms

Since in reality the data set is never complete to the point where infinitesimal  $\theta$  and  $l$  are reached, reconstruction is dependent on algorithms that provide reconstruction quality for a finite amount of pixels and acquisition angles. Another important factor besides quality is the computing time to reconstruct such a slice. This is dependent on the algorithm but also on its implementation and the available hardware. The algorithms presented here are back projection-based whereas iterative methods with forward projection will not be explained.

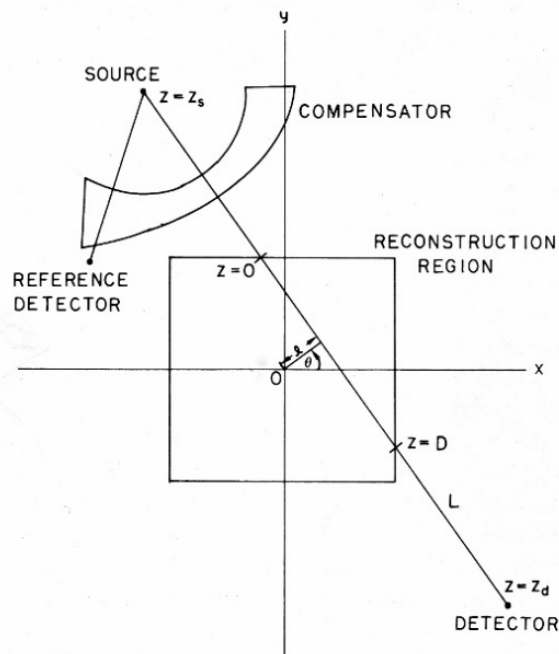


**Fig. 2.2.:** Computerized Tomography acquisition protocol [7, p. 30].  $\theta$  is the angle at which the acquisition happens,  $l$  the deviation to the side. The detector measures the intensity of the attenuated beam and together with a flat-field measurement, the attenuation  $A$  can be derived.

### Fourier Slice Theorem

The two algorithms presented here are based on the Fourier slice theorem which states that projecting a slice of a sample and do a Fourier transform is the same as a 2D Fourier transform of the sample space. Fig. 2.3 shows the 1D transform of the projections in the 2D Fourier space. As can be seen, the sampling gets lower with increasing distance from the origin. This corresponds to the high spatial frequencies, responsible for small details, like sharp edges. Underrepresentation of these frequencies leads to blurry images [13].

### Backprojection

Clearly the simplest reconstruction algorithm, it estimates the density (value of the attenuation coefficient  $\mu$ ) at a certain point by assigning every value in the a line the value of the line integral. This is done for all projection angles and the values are summed up [6, p. 125]. The problem stated in the section before is strongly visible with this reconstruction method: The image is very blurry due to the underrepresentation of high spatial frequencies. An example of this is shown in Fig. 2.4. Though unusable in practice, it lays the foundation for the next algorithm.

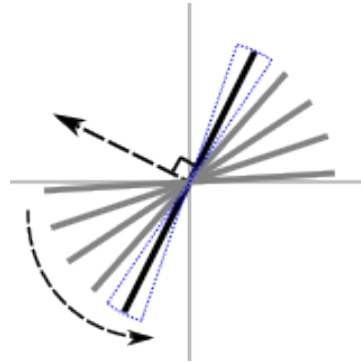
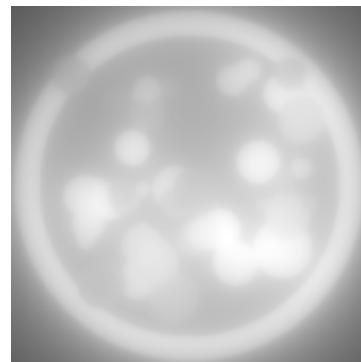


**Fig. 2.3.:** Fourier slice theorem. Shown is the 1D Fourier transform of the projections (gray and black lines) in the 2D Fourier space. A 2D back transformation would yield the sample space, but the undersampling in the outer regions is well visible (blue) [13].



(a) Original slice through the sample.



(b) Reconstruction of the same slice using BP.

**Fig. 2.4.:** An example of a backprojection using a phantom. The phantom depicts a capillary with spheres of different radii and density. The image is blurry and no details are visible with this method, making it unusable in practice.

## Filtered Back Projection

The simplest approach to solving the problem mentioned in the sections before, is to apply a filter to the 1D Fourier transforms of the projections (gray and black line in Fig. 2.3) before back projecting them [13]. This is to attenuate the low spatial frequencies such that they are equally represented after the back projection. The most commonly used filter is called *Ram-Lak* and is shown in Fig. 2.5. This filter's attenuation is linear with decreasing frequency and many other filters exist. An example of a reconstructed slice using FDK (Feldkamp, Davis & Kress), a 3D extension of the filtered back projection (FBP), will be shown in the Data Processing chapter in Fig. 5.6.

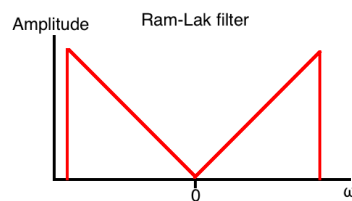


**Fig. 2.5.:** Ram-Lak filter that attenuates low spatial frequencies (around  $\omega = 0$ ) and lets high spatial frequencies pass [1]. This filter counteracts the underrepresentation of high spatial frequencies when using reconstruction algorithms that are based on the Fourier slice theorem.



# 3 LAB SETUP

This chapter should give an overview of the different hardware parts of the set up. All of them are mounted on a rail on an optical table such that the distances can be easily adjusted. In order to find points of optimization, the first 2 to 3 weeks of this thesis consisted of learning the following tasks:

1. Calculating and adjusting the setup geometry.
2. Learning how to align gratings by hand and laser as well as the fine-alignment with the motors.
3. Operating the detectors.
4. Combining the hardware in order to do phase stepping scans and determine the performance metrics of the system.

All of this was beneficial to the numerous grating tests that were performed during this time and it also led to the identification of the required capabilities for the operation software, explained in the next chapter.

## 3.1. Detector

Different detectors were used with this setup, but most frequently the Eiger R 1M from Dectris Ltd., because it provided very good image quality without any further processing. This detector has a photon detection range of 3.5 to 30 keV, a detection threshold can be set, its pixel size is  $75\ \mu\text{m}$  and the image size is  $1065 \times 1030$  pixels, resulting in an active surface of  $79.9 \times 77.1$  mm [8]. The almost square sensor area proved to be useful when handling samples in pipettes or capillaries that are mostly elongated along the vertical axis.

When creating setups for higher design energies (above 30 keV), a CdTe-based detector from Dectris was used, because its detection threshold could be adjusted to such high energy values.

### 3. Lab Setup

---

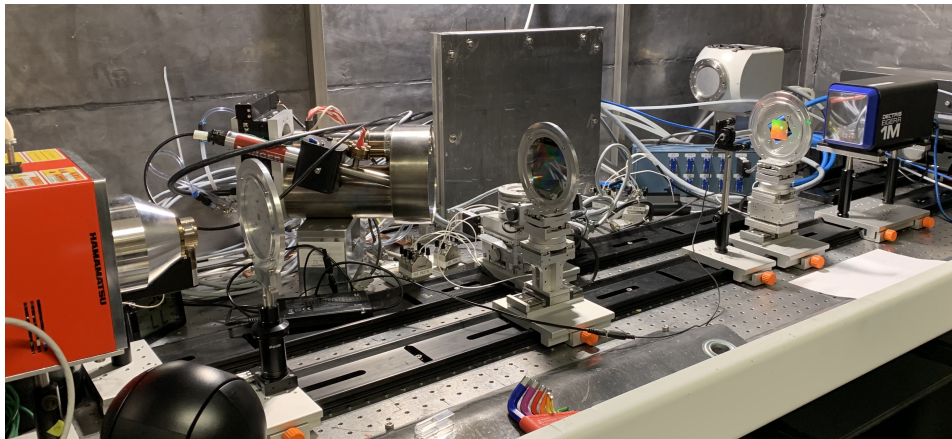


**Fig. 3.1.:** The setup as it was used during the course of this thesis. On the right the Dectris Eiger R 1M detector, the Hamamatsu L10101 microfocus source on the left and the three gratings on their respective motor towers in between on the rail.

Its pixel size was similar to that of Eiger, but it has a different field of view ( $256 \times 3094$  pixels or  $19.2 \times 232$  mm) with the longer side along the horizontal axis.

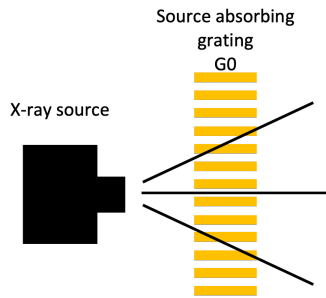
Lastly there was the X-ray sCMOS 16MP from *Photonic Science*. This detector's advantage is that it offers a much smaller pixel size which makes it possible to get even better spatial resolution of the sample.

## 3.2. Gratings

One of the centerpieces of the lab setup are the gratings. They are manufactured from silicon and the absorption gratings are then filled with gold. As explained in 2.4, a Talbot-Lau configuration is used. Important numbers for characterization of these gratings are duty cycle, aspect ratio and phase shifting properties. Duty cycle is defined as the ratio of grating ridge and grating period, aspect ratio as the ratio of trench depth and grating period and the phase shifting properties depend on the used energy and the trench depth. The gratings used during the process of this thesis had aspect ratios of up to 30 and introduced a phase shift of  $\pi$  or  $\pi/2$ .

As mentioned in 2.5.2, a smaller grating period is beneficial for reaching a smaller minimal detectable angle of refraction, so they should be preferred over gratings of larger period. Apart from the fact that they are more difficult to produce they add a difficulty to the geometry of the setup: As can be seen in Fig. 3.2a, the diverging beam passes easily through the central regions of the gratings but in the outer regions it passes through gold layers and therefore gets partially absorbed. The effect is a limited field of view, as shown in Fig. 3.2b. The easy

solution to this problem is to move the source grating further away, where the divergence has less of an influence. This was done during the grating test of the high aspect ratio gratings that is presented in appendix A. The more complex solution would be to bend the gratings with the right radius.



(a) The diverging beam of the X-ray source causes absorption in the outer parts of the grating. This limits the field of view.



(b) The transmission profile of a  $2\ \mu\text{m}$  grating. Apart from some inhomogeneities in the right part (circles), it can be seen that transmission is higher in the center part.

**Fig. 3.2.:** The diverging beam limits the field of view. An easy solution to this is to move the setup further away from the source where the beam shape is less conical.

### 3.3. Motorized Towers

Basic alignment of the gratings can be done by visual inspection as well as with the help of a laser. Pointing it onto the side where the grating is etched into the silicon wafer, the diffraction pattern can be assessed. In most cases one would want this pattern to be parallel to the earth, which in turn means that the grating structure is vertical to the earth.

The fine-tuning of the grating alignment happens with the help of motorized towers on which the gratings are mounted. These towers are customizable with linear motors and goniometers to reach many degrees of freedom at a very high resolution of motion. Since the sample has to be rotated and moved out of the detector area during the tomographic process, the sample itself is also placed on top of such a motor tower. The motor stages for the gratings were from SmarAct Inc., the one for the sample from HUBER Diffraktionstechnik GmbH & Co. KG.

### 3.4. X-Ray Source

Two microfocus sources were used with the setup, the L10101 from Hamamatsu Photonics and a prototype from Sigray Inc. The Hamamatsu source has a maximal tube voltage of 100 kV and a maximal current output of  $200\ \mu\text{A}$ . The source from Sigray has a significantly higher

power output, reaching up to 1200  $\mu\text{A}$  at up to 50 kV. The increased power is important since exposure time is an important factor for increasing the signal-to-noise ratio (SNR). With the introduction of the Sigray source during the time of this thesis and the boost in power that it provides, it should be possible to cut the exposure time sixfold in the future.

Another important feature of the X-ray source are the source sizes, since they influence the coherence. While the Hamamatsu tube has a source size of 10  $\mu\text{m}$  - 15  $\mu\text{m}$ , the Sigray prototype also includes a structured anode that creates an array of line sources, just like the source grating  $G_0$  would. This means that when making use of this structured anode,  $G_0$  is redundant and can be left out.

## 3.5. Placing and Alignment of Components

A geometry in accordance with 2.3 and 2.4 has to be chosen for the desired design energy. Shorter total lengths of the setup have an advantage when it comes to exposure time, longer distances between  $G_1$  and  $G_2$  ( $d$ ) increase the propagation length of the refracted beam and increase angular sensitivity, shown in 2.5.2.

Basic alignment of the 3 gratings is done using rulers and a laser pointer and  $G_1$  is subsequently aligned with the help of Moiré effects and the motor stage it sits on. Two types of fringes, produced by the overlapping of the reproduction of  $G_1$  with the analyzer  $G_2$ , can be observed:

1. Vertical fringes coming from a small deviation around the Talbot distance which is along the z-direction, also corresponding to the optical axis.
2. Horizontal fringes, caused by a rotation of one of the gratings around the z-axis.

The vertical fringe is visible from the beginning if alignment by hand and laser was done carefully. The goal is to make them completely vertical without diverging towards the top or the bottom, and then move  $G_1$  along the optical axis such that they get bigger and eventually disappear. This is the placement where the intensity pattern of  $G_1$  and the grating structure of  $G_2$  are congruent. Such a process is shown in Fig. 3.3. A set of printed gratings on overhead projector sheets proved to be a helpful tool for the interpretation of the observed fringes.

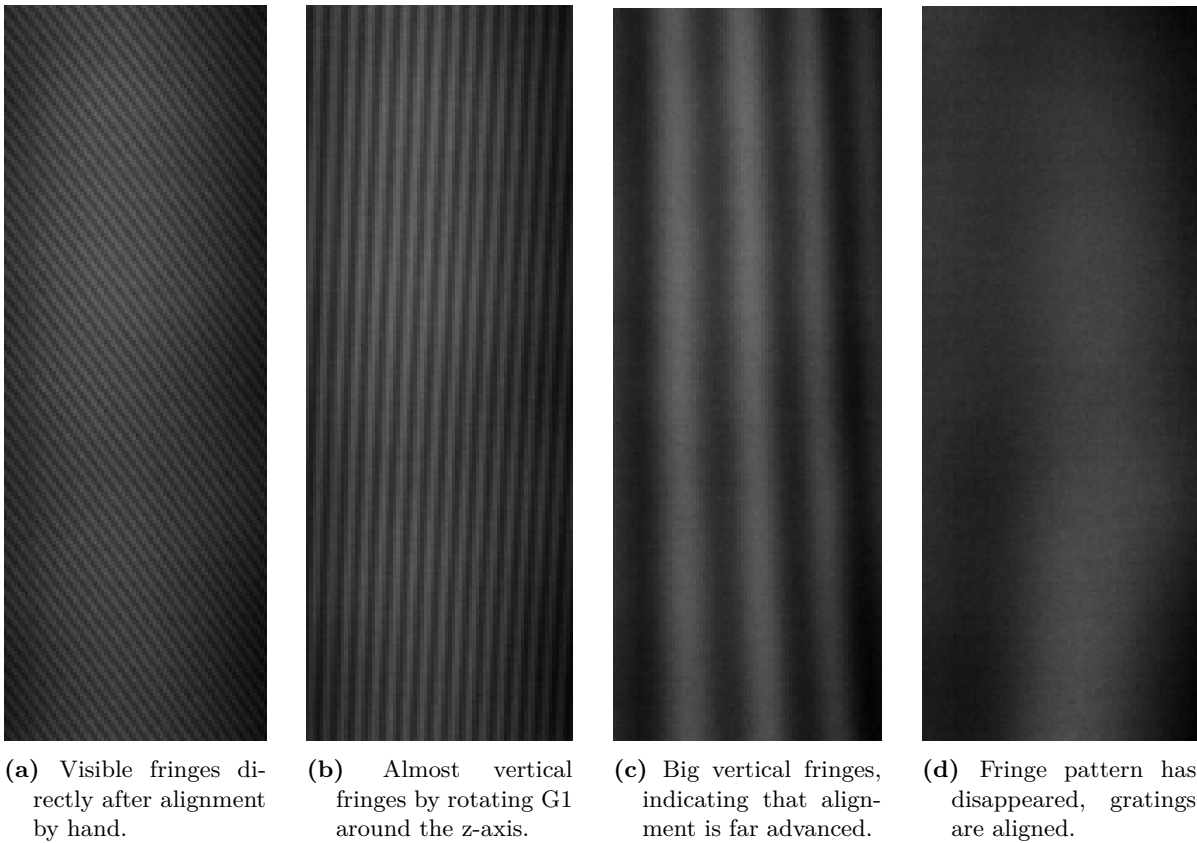


**Fig. 3.3.:** Grating alignment flow. The slight divergence towards the bottom seen in Fig. 3.3c can be corrected by rotating G1 around the  $x$ -axis.



# 4 OPERATION SOFTWARE

So far this setup had been operated with the help of a few scripts for operation of the detector as well as the motors, but most operations happened inside of Jupyter Notebooks following a low-level approach. The goals of the software development part were the following:

1. Implement a package that allows for high-level operation of the system.
2. Leave enough flexibility for future hardware components to be integrated in this package.
3. Reach a considerable reduction in acquisition times for the whole tomographic process.

This chapter tries to highlight where optimizations were made in order to reach these goals, what their impact was and why certain parts were left untouched. The full code can be found in the appendix.

## 4.1. Detector Operation

The detector is one of the key elements of such a setup. As mentioned in the previous chapter, the main detector in use was the Eiger R 1M by Dectris. After gaining experience in operating it with a class that had existed before, the functionality that should be expected from every detector operated with this setup was identified. This led to the creation of the interface `Detector` as seen in the class chart (Fig. 4.1). Separate classes for each detector were created and each class had to implement at least the functionality defined by the interface. This happens with the help of the attributes `client`, which are instances of the low level classes that were used before. This ensures that experienced users still get access to all low-level operations if necessary, with a call of `Eiger.client` in the case of the Eiger detector.

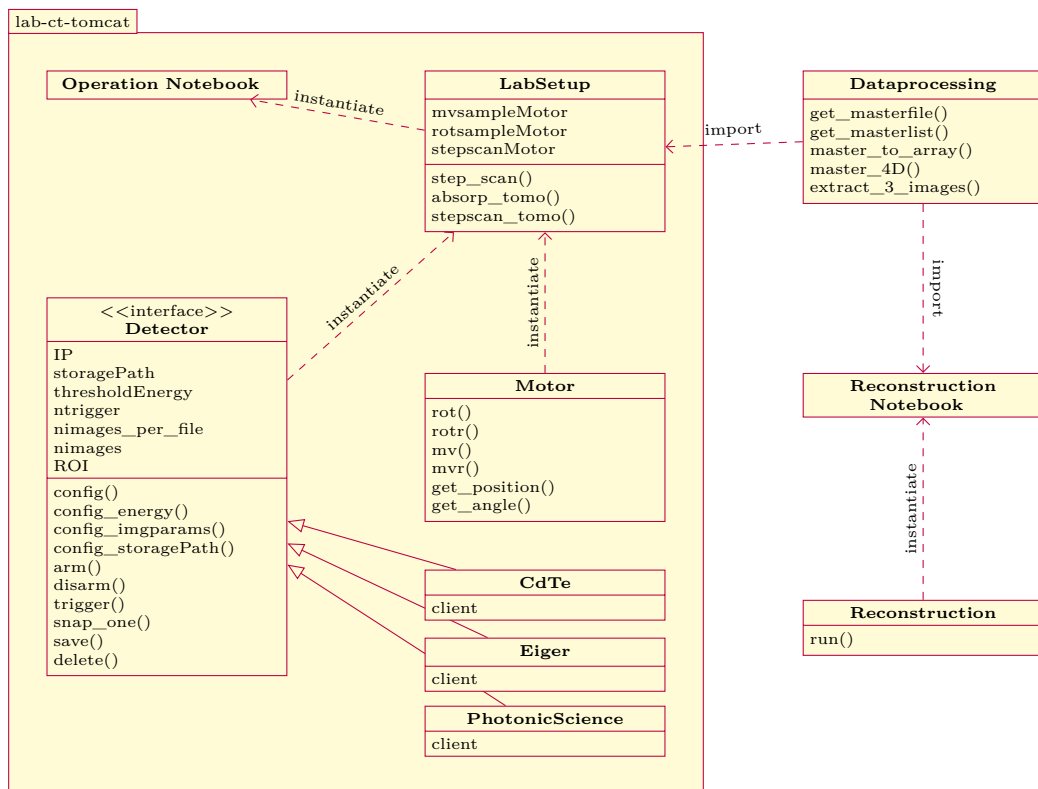


**Fig. 4.1.:** Class Chart. The interface `Detector` defines the functions and attributes that each detector should implement. `LabSetup` gets assigned 3 motors, a detector of a certain type and implements different functions that make use of all setup hardware. `Reconstruction` handles geometries and algorithms of the ASTRA toolbox. High-level operation happens in Jupyter Notebooks.

### 4.1.1. Acquiring Images with Eiger

This detector saves data in *HDF5* files. Every acquisition sequence consists of arming, sending a number of triggers for every image to be recorded, and disarming. For every such sequence a master file is created that contains a lot of metadata about the detector operation and links to data files, which contain one data set with one or more images each, as can be seen in Fig. 4.2.

The exact structure of these files is largely influenced by two detector parameters, *ntriggers* and *nimages\_per\_file*. The first determines how many images the detector expects to take in the next imaging sequence, the latter how large the data set in each data file should be [9]. As will be presented in the next section, this is of importance when operating the detector to avoid data loss and ensure a quick image acquisition with little overhead time.



**Fig. 4.2.:** File structure of *Eiger's HDF5* files.

### 4.1.2. Speeding up the Tomographic Process

So far every step scan series had been handled as one imaging series. This means that for every projection angle a master file linking to a data file with 5 images was transferred between the detector and the local storage. Master files are around 22.6 MB, while such a data file is around 14.2 MB. Since the main interest lies on the image, not the metadata, this discrepancy was undesired. Optimally the detector could acquire a whole tomographic data set as one imaging series, but the limiting factor is the buffer space on the detector side. Therefore a break is needed in between, where data saving happens and a new series is started [9].

Experimentally it was derived that overhead time for saving and clearing the buffer can be significantly decreased by combining 20 projection angles of 5 phase steps each and the safe detector operation at those parameters was demonstrated by acquiring several tomographic data sets.

Overhead time between the two methods was tested and the results can be found in Table 4.1. The code in List. 4.1 was the one that generated the faster results. It can be seen that overhead is very similar for the different exposure times but largely different from the process of saving

**List. 4.1:** Testing acquisition times with the Eiger detector. Shown here is the fast configuration where images are only saved after 20 projections or 100 images.

```

1  expTime = 5
2  n_im = 100
3
4  eiger.config_imgParams(nimages_per_file=5, ntrigger=n_im)
5
6  time1 = time.time()
7  eiger.arm(expTime)
8  for i in range(n_im):
9      eiger.trigger()
10 eiger.disarm()
11 eiger.save()
12 eiger.delete()
13 time2 = time.time()
14
15 timetot = time2 - time1
16 print(timetot)

```

**Table 4.1.:** Acquisition times for 100 images with different exposure times, once with saving every phase stepping scan of 5 images, once with saving only at the end.

|               | 20 proj. per masterfile | overhead | 1 proj. per masterfile | overhead |
|---------------|-------------------------|----------|------------------------|----------|
| 15 s exposure | 1523 s                  | 23 s     | 1590 s                 | 90 s     |
| 5 s exposure  | 520 s                   | 20 s     | 587 s                  | 87 s     |

only 1 projection angle per master file. This experiment was only conducted over 20 projection angles and a time difference of 70 s was reached. A typical number of projections for this setup would be 4 per degree, yielding a total of 1440 projections and a time saving of 5040 s or 1.4 h. This is a significant decrease compared to the prevalent method from before.

## 4.2. Motor Operation

The setup uses two different types of motor stages. One, the sample stage, is operated via the *epics* package for python, the others are operated through a custom written package. Though not implementing the exact same commands, both packages ensure that the python interpreter waits for the motor to reach its position. This is important to check because acquiring a projection or a flat-field while the sample is in movement, or not yet completely out of the detector area, should be avoided.

Instances of the motor classes all implement functions for relative movement, absolute movement and position feedback. They were left untouched since they already allowed high-level operation and worked very reliably.

### 4.3. The Lab CT as one Object

Acquisition of a whole tomographic data set may take several hours, therefore the risk of human error that leads to bad or incomplete data should be mitigated. The purpose of the `LabSetup` class is to implement the basic functionalities that are regularly used with this setup in such a way that they minimize the potential for human error and maximize time efficiency. This is done by implementing things learned during operation of the setup, like the imaging series optimization from section 4.1.2.

`LabSetup` gets assigned three motors, one for moving the sample out of the detector area to take flat-field projections, one to rotate the sample and one that moves the grating in order to perform the phase stepping scan. These procedures will generally be performed by the same motors therefore it makes sense to allocate those as defaults and avoid misassignment of such.

Further, `LabSetup` instantiates an object of a class that implements the detector interface. When instantiating an instance of `LabSetup`, the user can choose the detector that he would like to use. `LabSetup`'s methods rely on the fact that no matter which type of detector gets instantiated they can all be operated the same way, calling the same functions. This is the reason why the approach with the `Detector` interface was chosen. All detectors that are so far implemented support at least the functionality that is needed for the 2D operation of the setup. This means that all of them work reliably together with the `step_scan()` function that is defined in `LabSetup`. Functionality and ease of use of this `LabSetup` class was proven during several grating tests, including one where Zhitian Shi, a member of the microfabrication team, was able to operate the setup on his own in a very short period of time. The results of this grating test can be seen in appendix A.

For the case of the Eiger detector, where an enhancement of the operation was reached, functions were added to the `LabSetup` class that make use of those enhancements, either for a phase contrast tomography or for a pure absorption tomography. The tomographic scans by default require the user to visually inspect the movement of all involved motors, that the source is switched on and that the sample is placed on the sample motor stage. This again acts to minimize the risk of something going wrong during the scan and allows operation of the setup by a person who does not have a lot of experience. The system check can also be skipped in case several consecutive tomographies want to be acquired. Further, a log file will be created, containing all important information needed for further processing of the data set, which will be of importance when looking at tomographic reconstruction in chapter 5. This includes the detector threshold, exposure time, information about the scanned angles and info about the geometry. An example of how the `LabSetup` class can be used to acquire a tomography and

a single phase stepping scan can be seen in List: 4.2 and the output of the log file directly follows.

**List. 4.2:** Usage of the the LabSetup class to acquire a phase stepping tomography and two phase stepping scan with a sample. The distances of the setup can be passed with the constructor like it is seen here or can be added later. These are important properties that should be included in the log file. `sample_in` and `sample_out` are the motor positions where the sample is either inside or outside the frame.

```
1 base = '/sfs/X02DA/Data20/e15889/Maxim_LCT/data/2021/May/tomotryouts/'
2 lab = LabSetup(storagePath=base, detector='Eiger', source_sample_d=345,
3               sample_dect_d=160, vertcenter=410)
4
5 sample_in = -2000
6 sample_out = 6000
7 angles = np.linspace(0, 185, 185*4, endpoint=False)
8 lab.stepscan_tomo(storagePath=base+'tomo1', threshold=13000, sample_in=sample_in,
9                  sample_out=sample_out, angles_degrees=angles, expTime=15, stepsize=0.4)
10
11 # phase stepping scan with the sample
12 lab.mvsampleMotor.mv(sample_in) # move sample in
13 lab.step_scan(5, 0.4, 15, storagePath=base+'sample') # do a step scan for grating of
14               pitch 2 um
15
16 # phase stepping scan without the sample
17 lab.mvsampleMotor.mv(sample_out)
18 lab.step_scan(5, 0.4, 15, storagePath=base+'sample')
```

**List. 4.3:** logfile.txt from the tomographic data set acquired by the functions used in List.4.2

```
Threshold: 13000
Exposure Time: 15
Start Angle: 0.0
End Angle: 185.0
Number of Projections: 740
Source to Sample (rotaxis): 345mm
Sample (rotaxis) to Detector: 160mm
Acquisition Time: 56705.87584042549
```

## 4.4. Conclusions & Perspective

As a result of the implemented software framework it is now possible to operate the setup with a high-level approach, either from Jupyter Notebooks or directly from scripts. Not only does this help to mitigate the risk of something going wrong, it also opens new possibilities for other team members who are now, with very little instruction, able to use this setup as a tool for their own research. While facilitating this, it was also paid attention to the fact that more experienced users might want to make use of low-level operation: The already existing classes

were integrated into the framework and can still be called and used. In order to preserve the acquired data for the future, it was made sure that acquisition information gets stored together with it.

In the case of the Eiger detector, acquisition times for a whole tomographic data set were significantly cut by enhancing the file saving procedure. The gained knowledge was integrated into functions for tomographic scans and their successful operation was demonstrated with the acquisition of several such tomographies.

Possible next steps, in order to further enhance the operation, might include:

1. Cutting overhead times of the motors, since they were not looked at during the course of this thesis.
2. Cutting overhead times of the two other detectors and write enhanced tomography functions for them. As demonstrated with Eiger, this can make a significant difference.



# 5 DATA PROCESSING

This chapter will present how the quality of the interferometer can be assessed, as well as the handling and processing of large tomographic data sets. Specifically the retrieval of differential phase contrast and dark-field images will be discussed followed by their tomographic reconstruction. The two main goals were the following:

1. Create a collection of often used data processing functions and enhance their performance if necessary.
2. Implement an easy to use reconstruction class, capable of tomographic reconstruction of fan beam and cone beam shaped geometries.

## 5.1. Reading Detector Output

As mentioned in 4.1.2, the way the Dectris Eiger saves images is very specific. For further handling of the data it makes sense to import the projection data, or certain slices (detector rows) thereof, into an array of the dimensions ( $\#projections \times \#phases \times x \times y$ ). The values  $x$  and  $y$  are the pixel rows and columns of the detector and together form one projection image.

The challenge lies in finding a quick way to create said 4D array and handing it to the next step which is the retrieval of the 3 images, discussed in 5.3. In order to do this, one has to iterate over the files and merge the data sets. This is a lengthy process, even if only certain slices of the projection set should be imported. Therefore, 2 different approaches were chosen and their computing times were compared.

Data handling makes use of arrays from the *numpy* package. These data structures use fixed sizes such that the values can be stored closely together in storage and are quickly accessible. It was expected that one fast approach would be to initialize an array of this size with zero values and write the data sets one by one into it. This has the advantage that storage gets only allocated once and the values are directly written into the final structure, but the disadvantage

that its shape does not reveal if all values have been added. A second approach was to create a Python list of data sets and write them all into an array at the end. This has the disadvantage that before writing the data into the final structure, the list creation happens as an intermediate step. The advantage is that with this approach, the shape of the final array clearly states the actual amount of imported values. The results of this test can be seen in Table 5.1. Since this is mainly an I/O operation and no calculations are necessary, parallelization does not have a big influence. It was nevertheless tried to split the import of one master file among several processes, but the time saving was minimal. Therefore the parallelized approach was dropped in favor of list appending, which works reliably and its success is verifiable. In any case a repeated import should be avoided. This can be achieved by saving numpy binaries of imported slices on fast internal storage of the machine on which data processing happens. Since those binaries are often only a small fraction of the size of the whole data set they can be reloaded in a matter of seconds.

**Table 5.1.:** Computing times of two serial (zero initialization of the final array & list appending) and a parallel approach (distribute master files to different processes) to creating a 4D array from Eiger data. The data set contained 1440 projection angles and 2 slices were loaded. Parallelization did not save a lot of time and was therefore dropped in favor of the simplest approach which is list appending.

|                          | Computing Time [s] |             |
|--------------------------|--------------------|-------------|
|                          | 1st attempt        | 2nd attempt |
| zero initialization      | 251                | 233         |
| list appending           | 234                | 233         |
| splitting by core number | 205                | 204         |

Apart from the creation of the 4D array, the data processing collection includes functions that can extract single phase stepping scans from a master file, as well as create a 3D array from a pure absorption tomography. These work in similar ways, but data sets are significantly smaller therefore a speed-up was not tried.

## 5.2. Measuring Visibility & Angular Sensitivity

This setup is often used for testing of gratings produced at PSI and other institutions. Anyone operating the setup should be able to quickly analyze the most important performance metrics of *visibility* and *angular sensitivity*. For this, several functions were added to the collection, able of handling different inputs, making them very versatile and easy to use. Measurement of the visibility needs data from a phase stepping scan and functions were added that directly print a histogram that shows the visibility distribution with its peak as well as an image of the visibility, called the *visibility map*. Measurement of the angular sensitivity is done in a region

of the differential phase contrast image. This region should not include the sample but be constrained to the area of good visibility. A code example of a visibility measurement and angular sensitivity measurement is shown in List. 5.1, an example of an output can be found in Fig. A.2 of the appendix where a test of high aspect ratio bottom-up gold filled gratings is presented.

**List. 5.1:** Example of system operation and subsequent measurement of visibility and angular sensitivity. `lab` is an instance of `LabSetup` and the data processing functions are imported as `dp`.

```

1  steps = 5
2  grating_period = 2
3  stepsize = grating_period / steps
4  expTime = 120
5  distanceG1_G2 = 0.40
6  distanceSource_G1 = 0.60
7  distanceSource_sam = 0.48
8
9  lab.step_scan(steps, stepsize, expTime)
10 ff = dp.master_to_array(dp.get_masterfile(folder, seqID=7)) # step scan file had
    sequence ID 7
11 ref = ff[:, 200:500, 460:640] # choosing ROI
12
13 vis = dp.visibility(ref) # calculate visibility from a phase stepping scan
14 dp.plot_vishistogram(vis) # plot the visibility distribution
15 dp.plot_vismap(vis) # plot the visibility as an image
16
17 # step scan with sample
18 lab.step_scan(steps, stepsize, expTime)
19 sam = dp.master_to_array(dp.get_masterfile(folder, seqID=8)) # step scan file had
    sequence ID 8
20 sam = sam[:, 200:500, 460:640] # choosing ROI
21
22 amp, dpc, dci = dp.extract_3_images(sam, ref) # get dpc image for measuring angular
    sensitivity
23
24 # calculation of angular sensitivity takes all distances in m, small region of dpc
    image is passed
25 print(dp.angular_sensitivity(grating_period*10**(-6), distanceG1_G2, dpc[50:100,
    50:100], distanceSource_G1, distanceSource_sam))

```

### 5.3. Extracting the 3 Images

Every phase stepping scan in the 4D array from 5.1 must be analyzed and a set of projections (absorption contrast, differential phase contrast or dark field) must be generated. The implementation of FFT (fast Fourier transform) which numpy provides is very efficient as was shown with a comparison of extraction times, the results of which are shown in Table 5.2. The measurement was restricted to a maximum of 100 detector rows (*slices*), which means that from this data, 100 sinograms of each image type were created. This restriction was necessary since it is difficult to import many more rows from the raw data without the Python interpreter crashing. This is a task that should be easily parallelizable since it performs numerical

calculations on already loaded arrays, but the results do not demand an increase in speed as it is already reasonably fast.

**List. 5.2:** Example of the extraction of absorption contrast image and scattering image from a tomographic data set. The data processing functions are imported as `dp` and the extraction happens for the slices 400 to 420.

```

1 folder = '/mnt/test/Data20/Maxim_LCT/data/2021/April/tomography/murine_lung/25
  sec_4perdeg/'
2 masters = dp.get_masterlist(folder) # create a list with all masterfiles
3
4 myslice = np.s_[400:420] # choose which slices from detector data you want to import
5 dataset = dp.master_4D(masters=masters[1:-1], no_of_projections=740, sino_slice=
  myslice) # first and last masterfiles are flatfields
6 ff = dp.master_4D(masters[0], 1, myslices)
7
8 amp, dci = dp.extract_3_images(dataset, ff, amp=True, dpc=False, dci=True) # extract
  the images

```

**Table 5.2.:** Performance of the extraction was tested. The data set contained 740 projection angles and all 3 images were extracted on a machine with an Intel Xeon Gold 5222 (4 cores of 2 threads each) and 96 GB of RAM. Extraction is reasonably fast: For handling a limited number of slices from a data set, there is no need for a speed up.

|            | Computation Time [s] |             |
|------------|----------------------|-------------|
|            | 1st attempt          | 2nd attempt |
| 10 slices  | 1.27                 | 1.24        |
| 50 slices  | 5.93                 | 5.97        |
| 100 slices | 12.18                | 12.24       |

The results from such an extraction process can be seen in Fig. 5.1. These pictures depict a murine lung sample, placed in a capillary. The increased contrast in the dark field signal compared to the absorption contrast image is remarkable in this sample. More samples can be seen in Fig. A.3 and Fig. A.4 of the grating test in the appendix.

During the processing of a real sinogram from a tomography with the murine lung sample it was realized that the photon current provided by the Sigray source was strongly drifting over time. This leads to stripe artifacts after flat field correction as can be seen in Fig. 5.2. A straightforward approach to this would be to increase the frequency at which flat-fields are taken. This has the downside that tomographic scans would again become longer and depending on how fast the current changes it might not solve the problem. Nevertheless it should be mentioned that the `LabSetup` class from 4.3 was extended in order to take a flat field phase stepping scan after every 20th projection angle. This thesis ended before it was possible to determine the influence on the results. A different solution would be to explore dynamic flat-field correction with a database of flat-field images. The similarity of the projection and the flat-fields could be assessed and the best fitting flat-field would be used for correction.

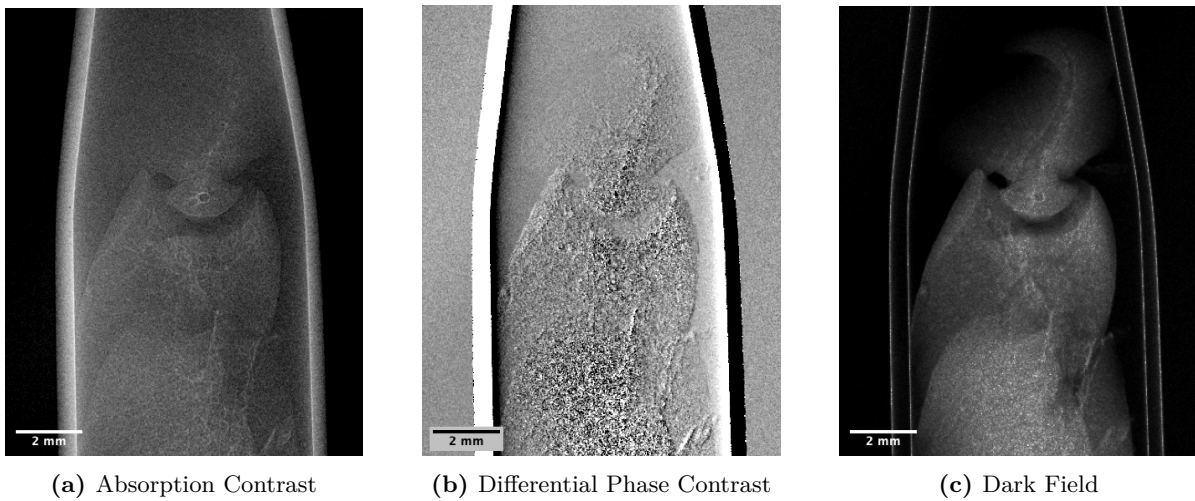


**Fig. 5.1.:** The results from processing the phase stepping data. The sample is a murine lung placed in a capillary. The contrast difference for the dark field signal compared to absorption contrast is remarkable in this sample. The magnification of  $M = 3$  was considered and the scale bars correspond to 2 mm in the sample plane.

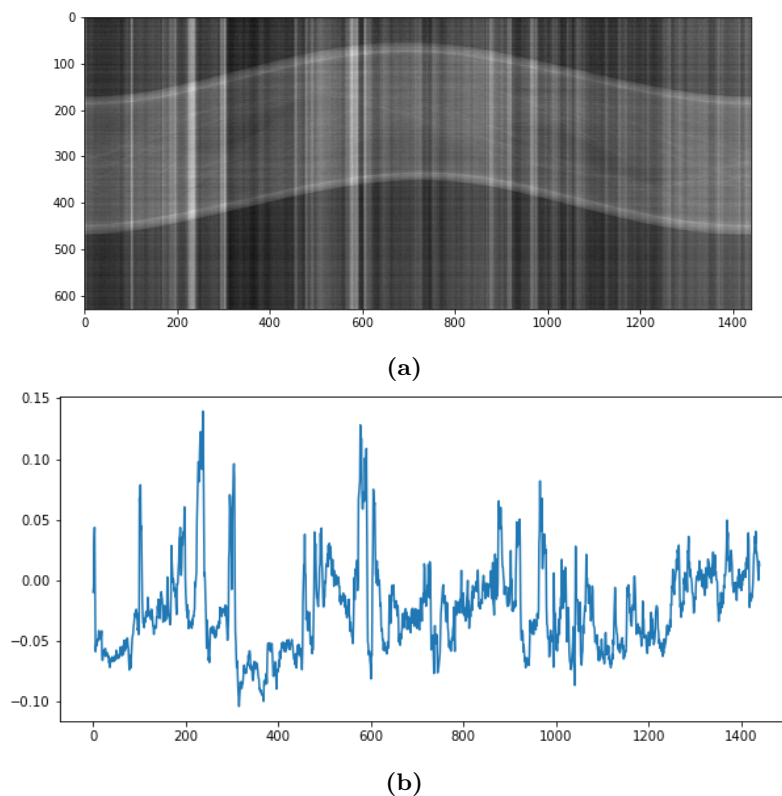


**Fig. 5.2.:** The figure in (a) shows a sinogram from a tomography with the Sigray source and murine lung sample. A total of 1440 projections was acquired (horizontal axis) over a time frame of 11 hours and after performing flat field correction with the same flat field for all projections the drift of the source was realized. The mean values of the lowest 100 pixels are shown in (b), indicating that the drift is very strong in the first 6 hours and gets better over time.

## 5.4. Tomographic Reconstruction

So far, only the *tomopy* package had been used for tomographic reconstruction from this setup. Tomopy uses CPU parallelization to reconstruct from projections taken with parallel geometries and is very well documented and user-friendly. It also includes a lot of useful tools for preprocessing the acquired data. Since tomopy was not able to handle reconstruction from cone beam shaped geometries, access to such algorithms was sought. The ASTRA toolbox is a package that implements a collection of sophisticated reconstruction algorithms, among them FBP & FDK (a 3D implementation of FBP) for cone and fan beam geometries as well as iterative methods, like SIRT. In addition to offering a wide variety of algorithms, many of them make use of the highly parallelizable Nvidia CUDA GPU architecture. The downside of ASTRA is, that it is poorly documented and its application is not user-friendly. For this reason, a reconstruction class was created that should make reconstruction with ASTRA as easy as it is with tomopy. Since the parallel geometry algorithms of the ASTRA toolbox were already integrated into tomopy in 2016, such that its users get access to GPU accelerated reconstruction within the same package [10], the focus was on reconstruction from fan-shaped and cone-shaped geometries.

### 5.4.1. The Reconstruction Class

In order for ASTRA to work properly it needs four basic objects:

**Volume geometry** An object describing the space in which the sample was placed.

**Projection geometry** Virtual representation of the real world setup dimensions.

**Volume data** An object in which the reconstructed data will be stored. It receives its dimensions from the volume geometry.

**Projection data** An object in which the data to be reconstructed – the sinograms – are stored.

Geometric magnification of a cone beam shaped setup is an issue that can be very confusing when trying to define a projection geometry in ASTRA. The standard origin is defined as the center of the sample and the reconstruction voxel size is  $1 \times 1 \times 1$ . For the geometry implementation in the Reconstruction class, a little trick presented by [14] is used to shift the origin into the detector plane, which makes the projection pixel the same size as the one from the reconstruction. All of the objects from the list above are used to create an algorithm object and such an object is also created when instantiating an object from the Reconstruction class using a cone beam shaped geometry. For the fan beam geometry it is a list of algorithm

objects that is created. This is due to the fact that the original fan beam geometry of ASTRA is only capable of handling one slice at a time. The fan beam handling of several slices is a significant improvement over using ASTRA directly and having to work with loops in the script or the Jupyter Notebook. A Reconstruction object has only one method, `run()`, that takes an optional argument `iterations` for iterative algorithms like SIRT.

**List. 5.3:** Example of how the Reconstruction class can be used to reconstruct slices from a number of sinograms. The goal was to make it as easy as it is in the tomopy package, therefore the direct comparison is given in the source code.

```

1 data = dp.make_sino(dci) # the data to be reconstructed are dark field sinograms
2
3 distance_source_origin = 235
4 distance_origin_detector = 685-235
5 detector_pixel_size = 0.075
6 angle_stop = 185
7 rotcenter = 565.7
8 vertcenter = 410
9
10 num_of_projections = 740
11 angles = np.linspace(0, angle_stop, num=num_of_projections, endpoint=False)
12 angles = angles * np.pi / 180 # ASTRA works with radians instead of degrees
13
14 # reconstruction using tomopy with the gridrec algorithms
15 recon = tomopy.recon(data,
16                     angles,
17                     rotcenter,
18                     algorithm='gridrec')
19
20 # reconstruction using a cone beam shaped geometry and SIRT with 200 iterations
21 recon = Reconstruction('cone',
22                       'SIRT3D_CUDA',
23                       rotcenter,
24                       angles,
25                       distance_source_origin,
26                       distance_origin_detector,
27                       detector_pixel_size,
28                       data,
29                       vertcenter=vertcenter)
30
31 data_recon = recon.run(iterations=200)

```

ASTRA by default assumes the rotation center to be in the center of the sinogram and in tomopy it is defined by a float passed to the reconstruction function, specifying the pixel where the rotation center is. The Reconstruction class is implemented such that the rotation center can now be passed the same way as in tomopy. This makes it easy to use both packages inside the same script. Further, the vertical difference between the source and the central slice of the detector can be passed as an optional argument. This is an important property when reconstructing data from strongly cone shaped geometries. Important to note is that the vertical difference between the sample and the X-ray source can not be adjusted. This would only be possible with a definition of the geometry using vectors. This is not only complicated but the fast FDK algorithm is so far not supported for these geometries. This means that

in order to be able to create the same geometry in ASTRA as in the real setup, the X-ray source and the sample have to be vertically aligned, while the detector may be slightly shifted up or down. The projection of a vertically aligned tip of a needle can be used to determine the central detector row. An example of how the Reconstruction class can be used is given in List. 5.3.

#### 5.4.2. Phantom Creation & Performance Testing

In order to test the performance of the package and determine how strongly the real setup is influenced by the diverging beam, several phantoms were created. The first one was a hollow cuboid with a square hole. It was derived from [14] and scaled to resemble the size of a real sample placed in the setup. A cuboid was chosen because the sharp edges show the influence of only partially attenuated beams very clearly. The phantom itself, together with three of its slices, are shown in Fig. 5.3. A simulated projection of the phantom was done using the exact geometry that was used in the real setup with the Sigray source. A look at the edges, as seen in Fig. 5.4, revealed that the blur caused by beams that only partially pass through the walls is significant and that reconstruction should definitely be done using a cone beam algorithm.

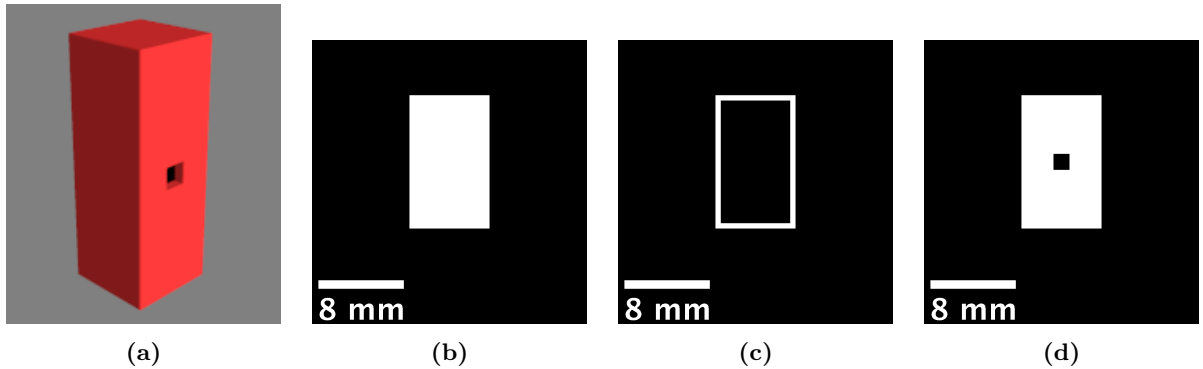


**Fig. 5.3.:** In order to determine how strong the influence of the diverging beam in the real setup is, a hollow box phantom was created. This phantom is inspired by [13] where picture (a) is from. The cuboid shape has the advantage that beams which only partially pass through the walls will be clearly visible as a blur on the otherwise sharp edge. Slices through the back wall (b), the middle (c) and the front wall (d) show the sharp edge and the scale bar shows that the size of the sample corresponds to the sample size of the murine lung from Fig. 5.1.

For testing how well the algorithms perform at reconstructing small details, a phantom was created that resembled the capillary from the murine lung sample from Fig. 5.1 and it was populated with 1000 spheres of randomized placement, radius and absorption coefficient. This phantom and one of its projections is shown in Fig. 5.5. Reconstruction of several slices using both FDK and SIRT were performed and the reconstruction results from this noise-free data are very convincing. Both reconstructions are shown in Fig. 5.6.

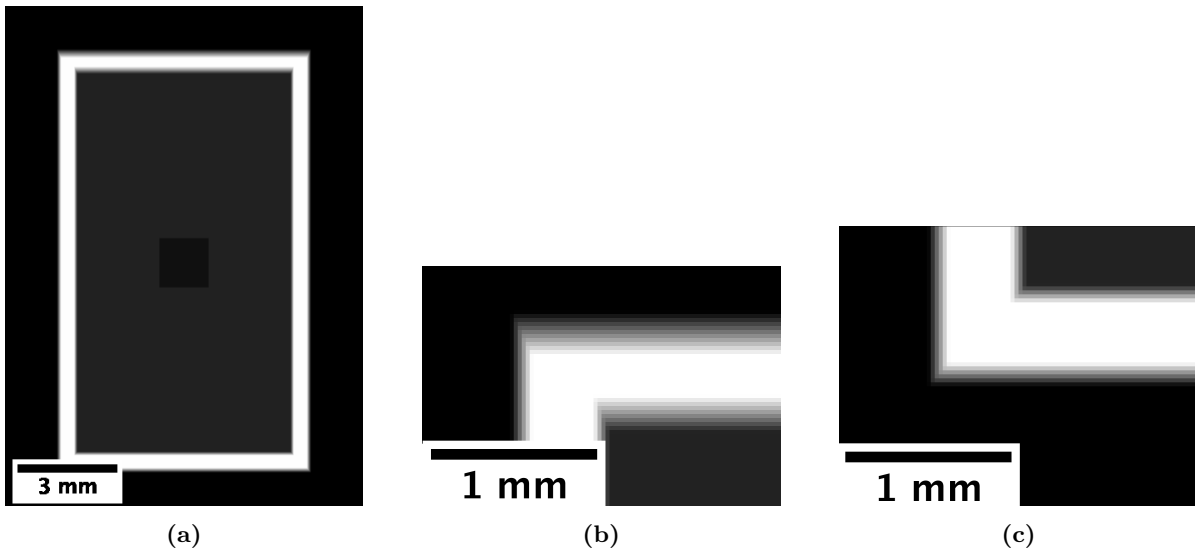


**Fig. 5.4.:** A simulated set of projections from the phantom in Fig. 5.3 was created with ASTRA and a cone beam geometry that corresponds to the real setup. Such a projection is shown in (a), clearly visible is the lower attenuation in the middle where the beam only passes through back and front wall (only the back wall in the case of the hole). A slight blur at the edges is also visible, especially when zooming into the edges (b) and (c). The diverging beam has a higher influence on the upper edge since the sample was placed above the vertical center (visible in Fig. 5.3).

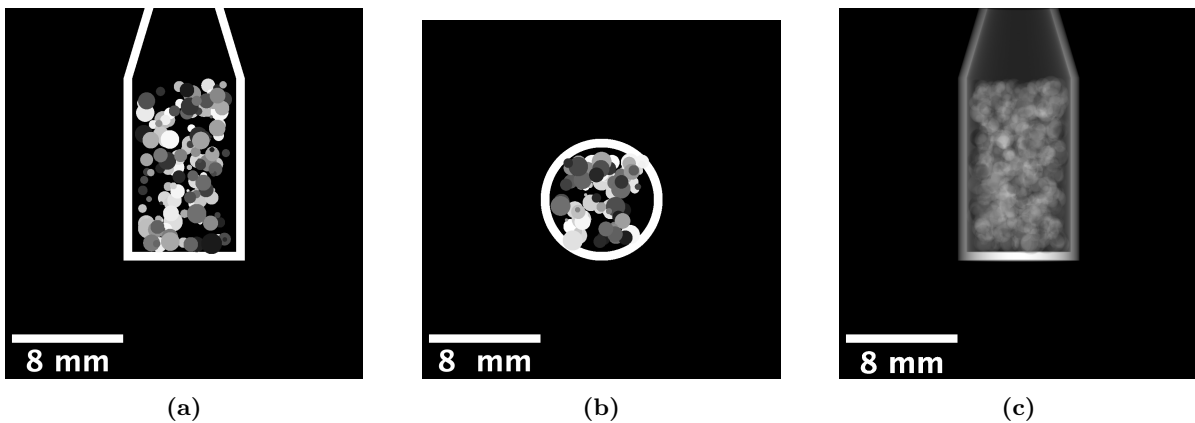


**Fig. 5.5.:** A phantom, resembling the murine lung sample from Fig. 5.1 in shape and size, was created in order to test the performance of the Reconstruction class. It consists of a cylindrical capillary, populated with 1000 spheres of randomized placement, density and radius. Slices through the side and the top of the phantom are shown in (a) and (b) respectively. The phantom was placed in a cone beam geometry of ASTRA and a set of simulated projections was created. One such simulated projection is shown in (c). Assuming it to be the size of the murine lung sample, the scale bar would correspond to 8 mm.

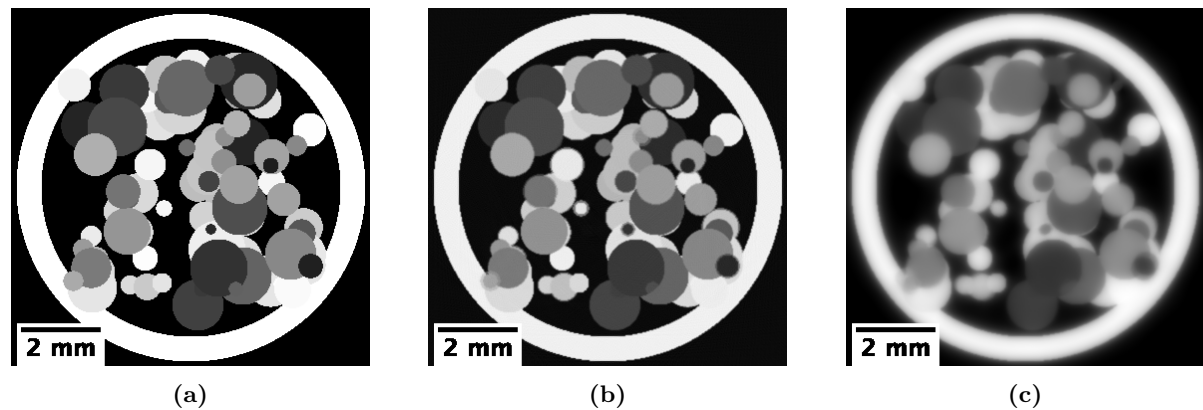


**Fig. 5.6.:** A total of 1440 projections (4 per degree) from Fig. 5.5c were used for reconstruction using a cone beam geometry created with the Reconstruction class. The original phantom slice is shown in (a), a reconstruction using FDK in (b) and a reconstruction using SIRT with 100 iterations in (c). Computing times for 100 slices were 3.4 s with FDK and 207 s with SIRT. With such a high number of projections and completely noise-free data, FDK is not only faster but also delivers superior reconstruction quality as is clearly visible from the images.

## 5.5. Conclusions & Perspective

Functions were created and collected to quickly load projections from raw acquisition data and retrieve absorption, differential phase and dark field images from them. Their performance was analyzed and improvements were tried where deemed necessary.

Tomographic reconstruction is now possible with 3D enhanced algorithms while the complexity for the user was kept to a level that is comparable to the software used before. With the help of phantoms it was shown that the chosen geometry corresponds to the real setup and that the quality of the reconstruction with high density and noise-free data is very good.

Further exploration of image retrieval from the phase stepping scans could include dynamic flat-field correction with a flat-field database. For tomographic reconstruction it could include the minimal number of projections needed for a desired spatial resolution. For this purpose the phantom with the spheres could be improved with smaller structures, a smaller range of densities and noise could be artificially added.

# 6

## CONCLUSIONS & PERSPECTIVE

During the course of this thesis I learned how X-ray grating interferometry works and how to operate the micro CT setup at the Paul Scherrer Institute. This led to the identification of points of improvement in the setup and an operation software package was created which makes it possible to operate the hardware components from within a single class. The function of the package was proven with the acquisition of several tomographic data sets and a grating test, the results of which can be found in appendix A. It was also demonstrated that by optimizing detector overhead time, a significant reduction in acquisition time is possible. The operation package allows an easy integration of further hardware components and its sustainability is supported by its placement on the PSI internal Git platform and a strong emphasis on complete Python docstrings. This not only helps the process of further development but the end-user also gets access to package information by a call of the `help()` function within the script or notebook. Further improvement of this package should include the cutting of overhead times in the motors as well as in the other detectors.

The created package for tomographic reconstruction and data processing follows the same principles of being well documented and easily accessible through PSI Git. It is now possible to access powerful tomographic reconstruction algorithms of the ASTRA toolbox with an easy-to-use class and also a function to create projections from a phantom was added. The functionality of the tomographic reconstruction class was demonstrated with the help of several phantoms, all of which are accessible via the corresponding Jupyter Notebooks. The collection for data processing contains all needed functions to assess the most important quality metrics of the interferometer and to prepare tomographic data for its reconstruction. This collection only contains the most basic functions and is expected to grow in the future. This could include dynamic flat-field correction for the image retrieval, which might help solve drift issues of the X-ray source. When it comes to tomographic reconstruction, the phantoms could be developed further by adding different structural features and make use of artificial noise in order to better assess the merits of each algorithm.



# A TESTING OF BOTTOM-UP GOLD FILLED HIGH ASPECT RATIO GRATINGS FOR X-RAY INTERFEROMETRY

The following section includes a grating test that was performed for high aspect ratio 1D absorption gratings. The gratings were produced using a bottom-up filling Au electrodeposition technique that yields in void-free gold fillings of the trenches. The grating tests included measurements of visibility and angular sensitivity, as well as the imaging quality assessment with several samples.

## A.1. Grating Tests

The performance of 1D-gratings was tested with an X-ray grating interferometer setup implemented at TOMCAT, Paul Scherrer Institute. The setup consisted of a microfocus X-ray source (Hamamatsu Photonics, model L10101) and a Dectris Eiger R 1M photon detector with a pixel size of  $75\ \mu\text{m}$ . The X-ray source was operated with a tube voltage of 42 kV and a current of  $200\ \mu\text{A}$ , providing a source size of  $10\ \mu\text{m}$ .

The interferometer was set up in Talbot-Lau configuration, with gratings  $G_0$ ,  $G_1$  and  $G_2$  being placed between the X-ray source and the detector, as shown in Fig. A.1. The purpose of the experiment was to measure the visibility in an X-ray interferometer [17] - a performance metric for grating interferometers, which depends on absorption properties of  $G_0$  and  $G_2$ . Better uniformity of the gold fillings translates into better absorption properties which allows to evaluate the manufacturing quality.

A design energy of 20 keV and the Talbot order 9 were chosen for the visibility tests. The phase shifting grating  $G_1$  was manufactured from silicon with a trench height of  $25\ \mu\text{m}$ , providing a phase shift of  $\pi$  at the given energy. Absorption gratings  $G_0$  and  $G_2$  were Au-filled with a height of  $60\ \mu\text{m}$ . All gratings –  $G_0$ ,  $G_1$ ,  $G_2$  – had a pitch of  $2\ \mu\text{m}$  and a duty cycle of 0.5 (trench

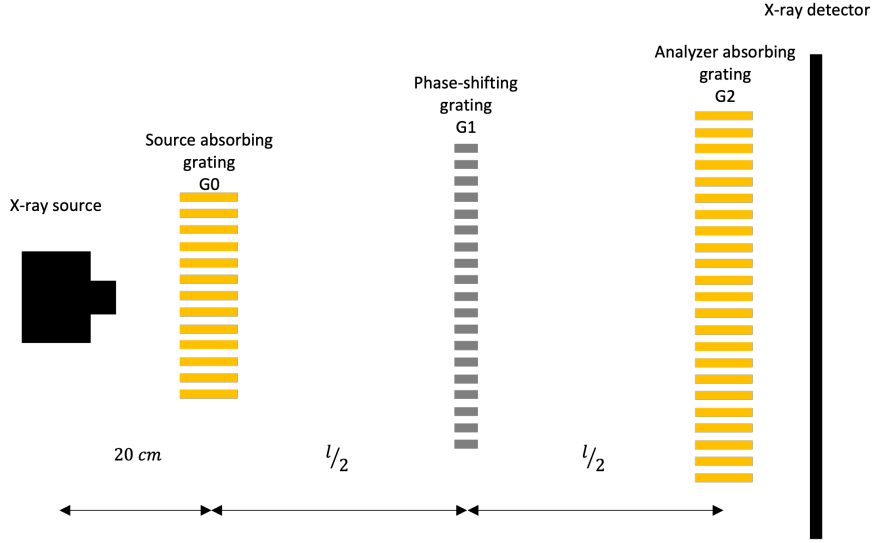


**Fig. A.1.:** A schematic of the symmetric X-ray grating interferometry setup, used for the quality assessment of the 1D gratings. Source- $G_0$  distance was 20 cm, and the detector was placed right behind  $G_2$ . For the case of the Talbot order 9, which was used for visibility measurements, the overall length  $l$  was 29 cm. For the case of the Talbot order 23, the overall length was 73.6 cm.

size of  $1\ \mu\text{m}$ . The visibility was measured using a phase stepping technique [23] [21], where  $G_2$  was moved in the grating plane perpendicular to the Au line structures.  $G_2$  was moved by a total of 5 steps over one grating period ( $0.4\ \mu\text{m}$  per step) and one image was taken for each step. The acquired visibility map can be seen in the Fig. A.2a, and the peak visibility of 21% was achieved, which is considered to be an indication of a good grating quality [17].

In order to visually assess the image quality of the tested gratings, two samples were alternately placed at a distance of 9.5 cm, upstream to  $G_1$ . The samples were chosen to fit in the area of a uniform visibility (Fig. A.2a, orange selection). For each sample, the stepping scan was performed [23], allowing to reconstruct three images with absorption, differential phase and dark-field contrast, respectively. The total magnification at the Talbot Order 9 was about 2, resulting in the effective pixel size of  $38\ \mu\text{m}$ .

Speaking of the imaging applications, angular sensitivity is another important performance metrics of the grating interferometer, which corresponds to the minimal refraction angle ( $\alpha_{min}$ ) that can be still detected by the interferometer. The refraction occurs after the interaction of X-rays with the features inside the sample. It was demonstrated in [21], that an angular sensitivity of less than 100 nrad is desirable to achieve good contrast. As for the case of our setup at the Talbot order 9, the angular sensitivity of 134 nrad was calculated, using the formula in [21] and calculating the standard deviation in the empty space of the differential

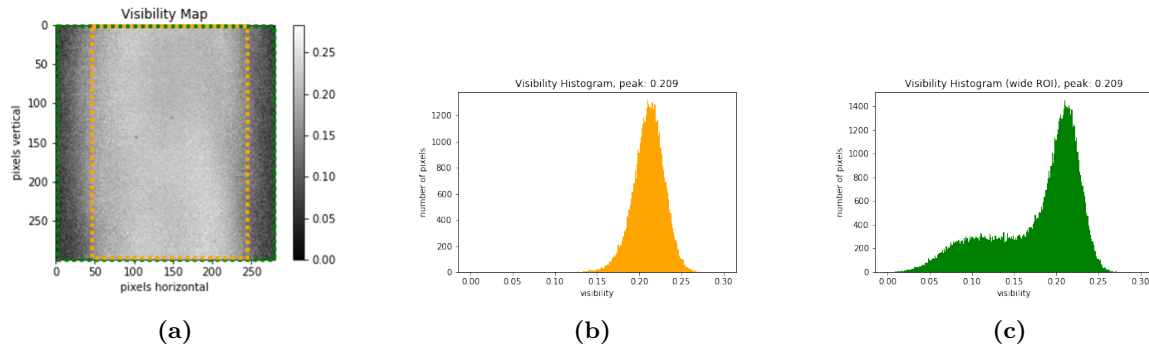


**Fig. A.2.:** The visibility map (a) indicates a uniform visibility distribution in the central region of interest (shown in orange), corresponding to the pronounced peak of 21% visibility at the histogram of individual pixels within this area (b). When enlarging the analyzed area in the horizontal direction (a, shown in green), the visibility drops rapidly towards the edges as seen from the histogram (c). This is due to the higher absorption at the edges of the  $G_2$  grating. Because of the high aspect ratio (60) and the high divergence of an X-ray beam generated by the laboratory X-ray source, the strong misalignment among X-rays and grating lines progressively increases the grating absorption at the edges. The usual solution for this issue is bending the grating to match the geometry of the X-ray wave front and improve their transmission.

phase contrast image. As angular sensitivity improves with using the higher distances, we decided to increase the  $G_0$ - $G_2$  distance up to 73.6 cm, to match the Talbot order 23. In addition, we modified the sample: the polystyrene balls were put in the ethanol to reduce the absorption contrast. The sample was placed upstream the  $G_1$  at the distance of 9 cm and the magnification of 1.6 was achieved. The imaging results shown in Fig. A.4a-c indicated an angular sensitivity of 90 nrad. This allowed to clearly highlight sample interfaces in the differential phase contrast, while showing no contrast in absorption mode.

## A.2. Conclusion

The performance of 1D gratings was tested by measuring the peak visibility of 21% in a Talbot-Lau X-ray interferometry setup. The recorded number indicates high manufacturing quality of the produced gratings, which was additionally confirmed by the good image quality of imaged samples, leading to high potential for such gratings in material science and biomedical applications.

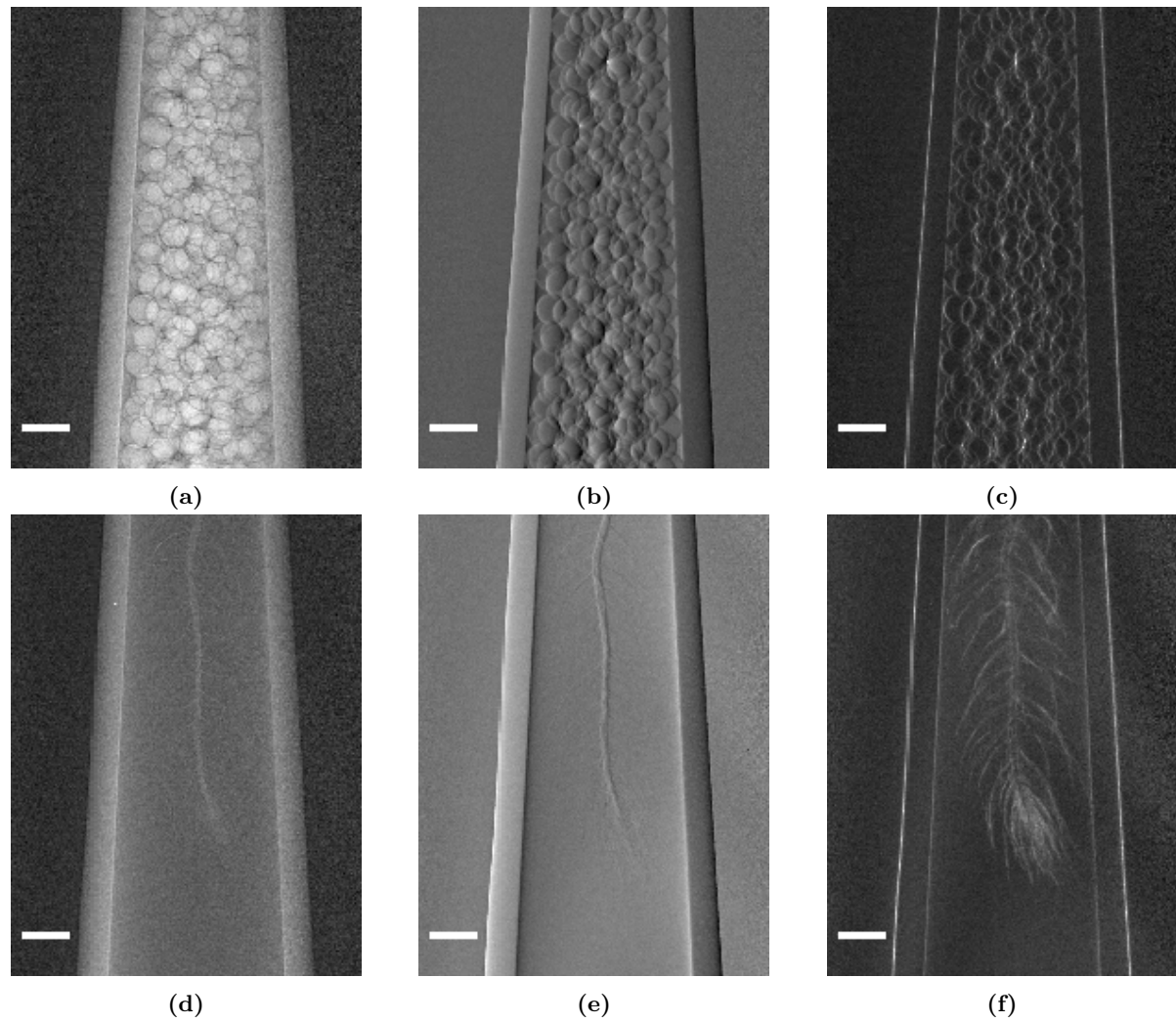


**Fig. A.3.:** Absorption (a, d), differential phase (b, e) and dark field (c, f) contrast images of two samples - polystyrene balls of 700  $\mu\text{m}$  and stem of Poaceae, respectively. The plant (Poaceae) sample is almost transparent in the absorption and phase contrast regimes, while the dark-field image clearly reveals more details of its inner structure. Scale bars at all images corresponds to 1 mm at the sample position as the magnification factor of 2 is taken into account.

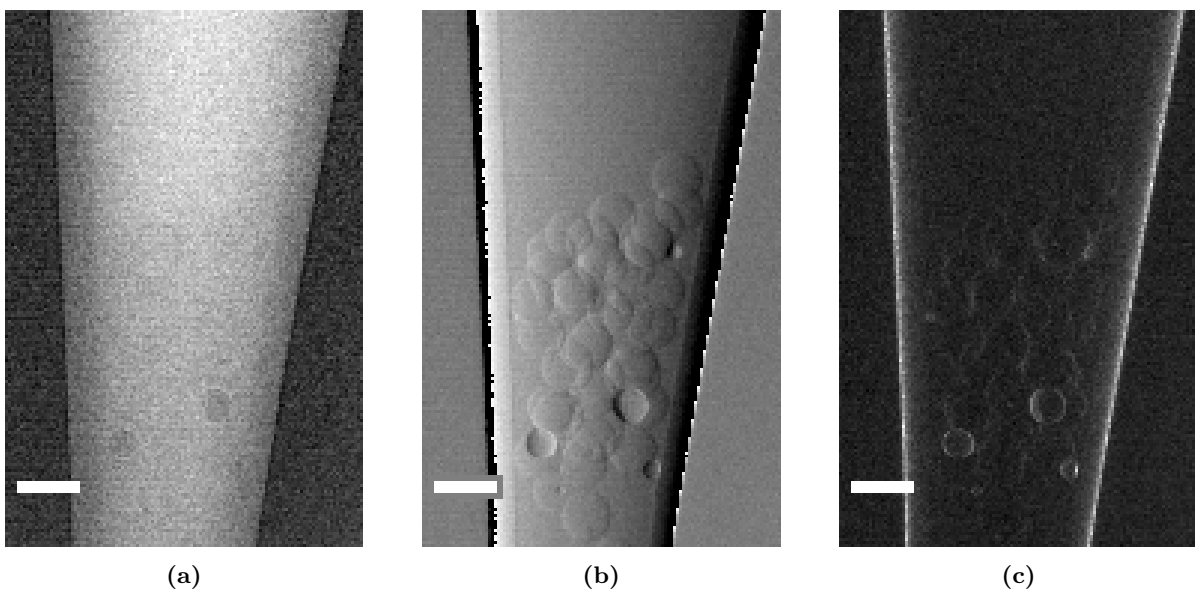


**Fig. A.4.:** Absorption (a), differential phase (b) and dark field (c) contrast images of the polystyrene balls with the diameter of  $700\ \mu\text{m}$  placed in the ethanol. The sample provides no contrast in the absorption mode while clearly revealing its structure in the differential phase image and, partially, - in the dark field image. Scale bars at all images corresponds to 1 mm at the sample position as the magnification factor of 1.6 is taken into account.



# B OPERATION & RECONSTRUCTION SOFTWARE

last update of this README file: 4. June 2021

This is a package to operate and process the data of the LAB CT setup at TOMCAT. A working clone of this package is currently located in 'Data20/Maxim\_LCT/Lionel\_dev/lab-ct\_tomcat/' and can for example be operated from cons-10.

please direct questions to [lionel.peer@gmail.com](mailto:lionel.peer@gmail.com)

## B.1. Requirements for operating the setup

- make sure the low level class DEigerClient is added to this folder (or make sure Detector.py gets access to this file)
- make sure the package smaract\_client\_py3 from [git.psi.ch](https://git.psi.ch) is cloned in the same folder (or just make sure that LabSetup.py gets access to this package)
- add or change smaract\_client\_py3.channel\_definition.py where you instantiate channels for the smaract motors (gratings towers) and for the epics motors (sample tower)
- make sure controls.remote\_detector for calling the CdTe detector is reachable by Detector.py
- make sure client.PS\_GSENSE\_Control for calling the PhotonicScience detector is reachable by Detector.py

## B.2. Requirements for operating the reconstruction

- conda environment with astra toolbox and tomopy, a currently working command that creates such an environment with the name 'tomoastra' is given below:

## B. Operation & Reconstruction Software

---

conda create -n tomoastra -c conda-forge -c astra-toolbox/label/dev python=3.6 astra-toolbox  
tomopy

- your workstation needs a Nvidia GPU in order to use of the Reconstruction class!

### B.3. Operation Software

List. B.1: Detector.py

```
1 import os
2 import glob
3 import h5py
4 import hdf5plugin
5 import matplotlib.pyplot as plt
6 import math
7 import numpy as np
8 import re
9 import time
10
11
12 # these must be provided
13 import DEigerClient as eigclient
14 import controls.remote_detector
15 import client.PS_GSENSE_Control as PS
16
17
18 class Detector:
19     """Detector Class defines methods to be implemented by different subclasses of
20     Detector.
21     It is kind of for illustration of how you should create functions and is
22     responsible for handling the variables that are common among all detectors.
23     """
24     def __init__(self, IP, storagePath, photonEnergy, thresholdEnergy, ROI=None,
25                 ntrigger=5, nimages=1, nimages_per_file=5, expTime=5):
26         """Instantiate and initialize a Detector.
27
28         Parameters:
29         IP (str): IP address of the detector server
30         storagePath (str): where to store the images
31         photonEnergy (int): targeted photon energies
32         thresholdEnergy (int): detector threshold photon energy
33         ROI (numpy.s_): 2D numpy slice object specifying region of interest
34         ntrigger (int): expected number of sent triggers
35         nimages (int): images to be taken for each trigger
36         nimages_per_file (int): images to be stored in one array
37         """
38         self.IP = IP
39         storagePath = os.path.join(storagePath, '') # add slash at end of path if
40         not already there
41         self.storagePath = storagePath
```

```

39     if not os.path.exists(self.storagePath):
40         os.makedirs(self.storagePath)
41     self.photonEnergy = photonEnergy
42     self.thresholdEnergy = thresholdEnergy
43     self.ntrigger = ntrigger
44     self.nimages = nimages
45     self.nimages_per_file = nimages_per_file
46     self.ROI = ROI
47     self.expTime = expTime
48
49     def config_energy(self, photonEnergy, thresholdEnergy):
50         """Reconfigure targeted photon energy and detector threshold energy.
51
52         Parameters:
53         photonEnergy (int): targeted photon energies
54         thresholdEnergy (int): detector threshold photon energy
55         """
56         self.photonEnergy = photonEnergy
57         self.thresholdEnergy = thresholdEnergy
58
59     def config_storage_path(self, storagePath):
60         """Reconfigure where to store the images.
61
62         Parameters:
63         storagePath (str): where to store the images
64         """
65         storagePath = os.path.join(storagePath, '')
66         self.storagePath = storagePath
67         if not os.path.exists(self.storagePath):
68             os.makedirs(self.storagePath)
69         print("Saving file to " + self.storagePath)
70
71     def config_imgParams(self, ntrigger, nimages, nimages_per_file):
72         """Reconfigure expected number of sent triggers and number of images taken
73         per trigger.
74
75         Parameters:
76         ntrigger (int): expected number of sent triggers
77         nimages (int): images to be taken for each trigger
78         nimages_per_file (int): how many pictures to store in one array
79         """
80         self.ntrigger = ntrigger
81         self.nimages = nimages
82         self.nimages_per_file = nimages_per_file
83
84     def config_ROI(self, ROI):
85         """Reconfigure region of interest of the detector.
86         Useless at the moment, but may help in the future
87
88         Parameters:
89         ROI (numpy.s_): 2D numpy slice object specifying region of interest
90         """
91         self.ROI = ROI

```

```
92     def snap_one(self, expTime, saving=True):
93         """Take one image with specified exposure time and save it to the detectors
94         storage path.
95
96         Parameters:
97         expTime (int): seconds of exposure time
98         """
99         self.expTime = expTime
100
101     def arm(self, expTime):
102         """Make detector ready for acquisition sequence.
103
104         Parameters:
105         expTime (int): seconds of exposure time
106         """
107         self.expTime = expTime
108
109     def trigger(self):
110         """Append an image to the acquisition sequence."""
111         print("Not implemented for parent class Detector.")
112
113     def disarm(self):
114         """End the acquisition sequence"""
115         print("Not implemented for parent class Detector.")
116
117     def delete(self):
118         """Delete all images on the server side."""
119         print("Not implemented for parent class Detector.")
120
121     def save(self):
122         """Save all images from the server to local storage."""
123         print("Not implemented for parent class Detector.")
124
125     def show(self, image, ROI=np.s_[:, :], vmin=None, vmax=None, figsize=None):
126         """Show an image.
127
128         Parameters:
129         image (numpy.array): 2D or 3D numpy array containing the image to be shown.
130         in case of 3D, the first image will be shown. try show_parallel().
131         ROI (numpy.s_): 2D numpy slice for zooming into specific region
132         vmin (float): min data range
133         vmax (float): max data range
134         figsize (float, float): float tuple, size in inches (fuck imperial!)
135         """
136         plt.subplots(figsize=figsize)
137         try:
138             if image.ndim is 3:
139                 plt.imshow(image[0][ROI], cmap='gray', vmin=vmin, vmax=vmax)
140             elif image.ndim is 2:
141                 plt.imshow(image[ROI], cmap='gray', vmin=vmin, vmax=vmax)
142         except:
143             print("This image does not have the right shape. Enter a 2D or 3D numpy
144             array")
```

```

143     def show_parallel(self, images, ROI=np.s_[:::], vmin=None, vmax=None, figsize=
None):
144         """Show several images next to each other.
145
146         Parameters:
147         image (numpy.array or list): 3D numpy array containing images to be shown or
list of 2D arrays
148         ROI (numpy.s_): 2D numpy slice for zooming into specific region
149         vmin (float): min data range
150         vmax (float): max data range
151         figsize (float, float): float tuple, size in inches (fuck imperial!)
152         """
153         if type(images) is list:
154             no_plots = len(images)
155         elif type(images) is np.ndarray:
156             no_plots = images.shape[0]
157
158         fig, axs = plt.subplots(1, no_plots, figsize=figsize)
159         for i in range(no_plots):
160             axs[i].imshow(images[i][ROI], cmap='gray', vmin=vmin, vmax=vmax)
161         plt.show()
162
163     class Eiger(Detector):
164         """Create an instance of Eiger if you want to use this detector without doing
any phase stepping or even tomography."""
165
166         def __init__(self, storagePath, IP="129.129.99.92", photonEnergy=20000,
thresholdEnergy=10000, ntrigger=100, nimages=1, nimages_per_file=5, init=False):
167             """Instantiate and initialize an Eiger Detector.
168
169             Parameters:
170             IP (str): IP address of the detector server
171             storagePath (str): where to store the images
172             photonEnergy (int): targeted photon energies
173             thresholdEnergy (int): detector threshold photon energy
174             ntrigger (int): expected number of sent triggers
175             nimages (int): images to be taken for each trigger
176             nimages_per_file (int): how many images to store in one array
177             """
178             super(Eiger, self).__init__(storagePath=storagePath, IP=IP, photonEnergy=
photonEnergy, thresholdEnergy=thresholdEnergy, ntrigger=ntrigger, nimages=
nimages, nimages_per_file=nimages_per_file)
179             self.client = eigclient.DEigerClient(host=self.IP)
180             if init == True:
181                 print("Reinitializing the Eiger Detector, setting seq ID to 1...")
182                 self.client.sendDetectorCommand("initialize")
183             else:
184                 print("Configuration of Eiger Detector...")
185             self.client.setDetectorConfig("ntrigger", self.ntrigger)
186             self.client.setDetectorConfig("nimages", self.nimages)
187             self.client.setDetectorConfig("photon_energy", self.photonEnergy)
188             self.client.setDetectorConfig("threshold_energy", self.thresholdEnergy)
189             self.client.setFileWriterConfig("nimages_per_file", self.nimages_per_file)

```

## B. Operation & Reconstruction Software

---

```
190         print("Photon energy set to " + str(self.client.detectorConfig("
191 photon_energy")["value"]) + " eV")
191         print("Threshold energy set to " + str(self.client.detectorConfig("
192 threshold_energy")["value"]) + " eV")
192         print("ntrigger set to " + str(self.client.detectorConfig("ntrigger")["value
193 "]))
193         print("nimages set to " + str(self.client.detectorConfig("nimages")["value"
194 ]))
194         print("nimages_per_file set to " + str(self.client.fileWriterConfig("
195 nimages_per_file")["value"]))
195         print("Saving files to " + self.storagePath)
196
197     def reinitialize(self):
198         """Reset the sequence ID to 1 and keep detector parameters."""
199
200         print("Reinitializing the Eiger Detector, setting seq ID to 1...")
201         self.client.sendDetectorCommand("initialize")
202         self.__init__(self.storagePath, self.IP, self.photonEnergy, self.
203 thresholdEnergy, self.ntrigger, self.nimages, self.nimages_per_file)
204
205     def config_energy(self, thresholdEnergy, photonEnergy=None):
206         """Reconfigure targeted photon energy and detector threshold energy.
207
208 Parameters:
209 thresholdEnergy (int): detector threshold photon energy
210 photonEnergy (int): targeted photon energies
211 """
212         super(Eiger, self).config_energy(photonEnergy=photonEnergy, thresholdEnergy=
213 thresholdEnergy)
214         print("Reconfiguration of Eiger Detector...")
215         if photonEnergy is not None:
216             self.client.setDetectorConfig("photon_energy", self.photonEnergy)
217             self.client.setDetectorConfig("threshold_energy", self.thresholdEnergy)
218             print("Photon energy set to " + str(self.client.detectorConfig("
219 photon_energy")["value"]) + " eV.")
220             print("Threshold energy set to " + str(self.client.detectorConfig("
221 threshold_energy")["value"]) + " eV.")
222
223     def config_imgParams(self, ntrigger, nimages, nimages_per_file):
224         """Reconfigure expected number of sent triggers and number of images taken
225 per trigger
226
227 Parameters:
228 ntrigger (int): expected number of sent triggers
229 nimages (int): images to be taken for each trigger
230 nimages_per_file (int): how many images to store in one array
231 """
232         if ntrigger > 120:
233             print('Recommended to go to lower ntrigger value. This can lead in the
234 detector hanging up and data loss.')
235         super(Eiger, self).config_imgParams(ntrigger=ntrigger, nimages=nimages,
236 nimages_per_file=nimages_per_file)
237         print("Reconfiguration of Eiger Detector...")
238         self.client.setDetectorConfig("ntrigger", self.ntrigger)
```

```

232     self.client.setDetectorConfig("nimages", self.nimages)
233     self.client.setFileWriterConfig("nimages_per_file", self.nimages_per_file)
234     print("ntrigger set to " + str(self.client.detectorConfig("ntrigger")["value
    ]))
235     print("nimages set to " + str(self.client.detectorConfig("nimages")["value
    ]))
236     print("nimages_per_file set to " + str(self.client.fileWriterConfig("
    nimages_per_file")["value"]))
237
238     def arm(self, expTime):
239         """Arm the Eiger for passed exposure time.
240
241         Parameters:
242         expTime (float): exposure time in seconds
243         """
244         super(Eiger, self).arm(expTime)
245         self.client.setDetectorConfig("frame_time", self.expTime + 0.000020)
246         self.client.setDetectorConfig("count_time", self.expTime)
247         print("Arming the Eiger Detector...")
248         retVal = self.client.sendDetectorCommand("arm")
249         if type(retVal) is not dict:
250             print("EIGER control hang and got probably reinitialized")
251             sys.exit("EIGER hang")
252         self.last_sq_id = retVal['sequence id']
253         print("Sequence ID is: " + str(self.last_sq_id))
254
255     def disarm(self):
256         """Disarm the Eiger. End acquisition sequence."""
257         time.sleep(0.2)
258         self.client.sendDetectorCommand("disarm")
259         print("Eiger Detector disarmed")
260
261     def trigger(self):
262         """Acquire image for acquisition sequence."""
263         self.client.sendDetectorCommand("trigger")
264
265     def snap_one(self, expTime, saving=True):
266         """Take one image with given exposure time
267
268         Parameters:
269         expTime (float): exposure time in seconds
270         saving (bool): default True, specifies if detector should save() and delete
    ()
271
272         Return:
273         storagePath (str): where image was saved
274         last_sq_id (int): the sequence id of the last image
275         """
276         super(Eiger, self).snap_one(expTime)
277         self.arm(self.expTime)
278         self.trigger()
279         self.disarm()
280         if saving:
281             self.save()

```

```

282         self.delete()
283         return self.storagePath, self.last_sq_id
284
285     def save(self, storagePath=None):
286         """Save all images from the server to storagePath or to default storage path
287         of detector.
288
289         Parameters:
290         storagePath (str): default is self.storagePath
291         """
292         time.sleep(1)
293         matching = self.client.fileWriterFiles()
294         old_path = self.storagePath
295         if storagePath is not None:
296             self.config_storage_path(storagePath)
297         for fn in matching:
298             self.client.fileWriterSave(fn, self.storagePath)
299         self.config_storage_path(old_path)
300
301     def save_onlydata(self):
302         """Save only the _data files created by Eiger to specified storage Path."""
303         time.sleep(1)
304         matching = self.client.fileWriterFiles()
305         contains_data = lambda x: "_data_" in x
306         matching = list(filter(contains_data, matching))
307         for fn in matching:
308             self.client.fileWriterSave(fn, self.storagePath)
309
310     def delete(self):
311         """Delete all images on the server side."""
312         time.sleep(1)
313         matching = self.client.fileWriterFiles()
314         for fn in matching:
315             self.client.fileWriterFiles(fn, method='DELETE')
316
317     def master_to_array(self, file):
318         """Return 3D numpy array of images stored in master file.
319
320         Parameters:
321         file (str): path to h5 master file containing images
322         """
323         with h5py.File(file, 'r') as f:
324             arr = np.array(f['entry']['data']['data_000001'])
325             for i in list(f['entry']['data'].keys())[1:]:
326                 try:
327                     arr = np.append(arr, f['entry']['data'][i], axis=0)
328                 except:
329                     print("Some images might not have been added due to corrupted
330                     file links")
331                     break
332             return arr
333
334     def get_masterfile(self, sequence_id):
335         """Return path to master file with specified sequence ID.

```

```

334
335     Parameters:
336     sequence_id (int): which file to get path from
337
338     Return:
339     path (str): path to searched master file
340     """
341     contains_id = lambda x: ("_" + str(sequence_id) + "_master") in x
342     file = list(filter(os.path.isfile and contains_id, glob.glob(self.
storagePath + '*')))
343     return file[0]
344
345 class CdTe(Detector):
346     """Create an instance of CdTe if you want to use this detector without doing any
phase stepping or even tomography."""
347
348     def __init__(self, storagePath, IP="129.129.99.75", photonEnergy=None,
thresholdEnergy=20000, thresholdEnergy2=50000, ntrigger=10):
349         """Instantiate CdTe.
350
351         photonEnergy (int): this detector does not have this parameter.
352         """
353         super(CdTe, self).__init__(IP=IP, storagePath=storagePath, photonEnergy=
photonEnergy, thresholdEnergy=thresholdEnergy, ntrigger=ntrigger)
354         self.thresholdEnergy2 = thresholdEnergy2
355         self.seqID = 1
356         print("Initialization of CdTe Detector...")
357         self.client = controls.remote_detector.RemoteDetector(IP, storage_path=self.
storagePath, photon_energy=[self.thresholdEnergy, self.thresholdEnergy2])
358         print("Threshold 1 set to", self.thresholdEnergy)
359         print("Threshold 2 set to", self.thresholdEnergy2)
360
361     def snap_one(self, expTime, saving=True):
362         """Take one image with exposure time: expTime"""
363         super(CdTe, self).snap_one(expTime)
364         self.client.setNTrigger(1)
365         self.client.arm()
366         self.client.trigger(self.expTime)
367         print('seqID:', self.seqID)
368         if saving:
369             self.save()
370
371     def arm(self, expTime):
372         """Arm CdTe detector with given exposure time."""
373         super(CdTe, self).arm(expTime)
374         self.client.arm()
375         print('seqID:', self.seqID)
376
377     def trigger(self):
378         """Send trigger to CdTe detector."""
379         self.client.trigger(self.expTime)
380
381     def disarm(self):
382         """Disarm CdTe detector."""

```

```

383         self.client.disarm()
384
385     def config_imgParams(self, ntrigger, nimages, nimages_per_file):
386         """File saving with CdTe should be further explored. ntrigger is the only
387         parameter at the moment that has an influence here."""
388         super(CdTe, self).config_imgParams(ntrigger=ntrigger, nimages=nimages,
389         nimages_per_file=nimages_per_file)
390         self.client.setNTrigger(ntrigger)
391
392     def config_energy(self, thresholdEnergy1, thresholdEnergy2):
393         """Config energy thresholds for CdTe. This detector has no parameter
394         photonEnergy."""
395         super(CdTe, self).config_energy(None, thresholdEnergy1)
396         self.thresholdEnergy2 = thresholdEnergy2
397         self.client.set_energy_and_thresholds([self.thresholdEnergy, self.
398         thresholdEnergy2])
399
400     def save(self):
401         """Save files in the master file convention with the sequence id."""
402         self.client.save('master_' + str(self.seqID) + '.h5')
403         self.seqID += 1
404
405     def delete(self):
406         """No such function necessary here."""
407         pass
408
409     def config_storage_path(self, storagePath):
410         """Reconfigure where to store the images.
411
412         Parameters:
413         storagePath (str): where to store the images
414         """
415         super(CdTe, self).config_storage_path(storagePath)
416         self.client.storage_path = self.storagePath
417
418     def get_masterfile(self, sequence_id):
419         """Return path to master file with specified sequence ID
420
421         Parameters:
422         sequence_id (int): which file to get path from
423
424         Return:
425         path (str): path to searched master file
426         """
427         contains_id = lambda x: ("master_" + str(sequence_id)) in x
428         file = list(filter(os.path.isfile and contains_id, glob.glob(self.
429         storagePath + '*')))
430         return file[0]
431
432     def master_to_array(self, file, threshold):
433         """Extract dataset from master file."""
434
435         with h5py.File(file, 'r') as f:
436             arr = []

```

```

432         if threshold is 1:
433             th = 'threshold_0'
434         else:
435             th = 'threshold_1'
436
437         for i in list(f['entry']['data'][th].keys()):
438             try:
439                 arr.append(f['entry']['data'][th][i][()])
440             except:
441                 print("Some images might not have been added due to corrupted
file links")
442                 break
443         return np.asarray(arr)
444
445 class PhotonicScience(Detector):
446     """Instantiate this one if you want to use the Photonic Science detector."""
447
448     def __init__(self, storagePath, IP='129.129.99.116', port=50000):
449         """Initialize PhotonicScience detector."""
450         super(PhotonicScience, self).__init__(IP=IP, storagePath=storagePath,
photonEnergy=None)
451         self.port = port
452         self.seqID = 1
453         filename = 'master_' + str(self.seqID)
454         self.client = PS.PSCamera(host=self.IP, port=self.port, camera="
FKGSense_bin1x1")
455         self.client.CameraSetup(self.expTime, self.storagePath, filename, self.
nimages)
456
457     def config_energy(self, photonEnergy, thresholdEnergy):
458         super(PhotonicScience, self).config_energy(photonEnergy, thresholdEnergy)
459         # has this even a threshold?
460
461     def config_imgParams(self, ntrigger, nimages, nimages_per_file):
462         super(PhotonicScience, self).config_imgParams(ntrigger, nimages,
nimages_per_file)
463
464     def arm(self, expTime):
465         super(PhotonicScience, self).arm(expTime)
466
467     def disarm(self):
468         pass
469
470     def trigger(self):
471         pass
472
473     def snap_one(self, expTime):
474         super(PhotonicScience, self).snap_one(expTime)
475
476     def save(self):
477         pass
478
479     def delete(self):
480         pass

```

List. B.2: LabSetup.py

```
1 import time
2 import numpy as np
3 import numpy.fft as npfft
4 import matplotlib.pyplot as plt
5
6 import Detector as dect
7
8 import warnings
9 with warnings.catch_warnings():
10     warnings.filterwarnings("ignore", category=RuntimeWarning)
11     warnings.filterwarnings("ignore", category=UserWarning)
12     from smaract_client_py3.channel_definition import *
13
14 class LabSetup:
15     """Lab Setup implements methods that use all hardware parts.
16     Initialise this class as soon as you need to use motors.
17     Otherwise, the Detector.py file may be good enough.
18     """
19
20     def __init__(self, storagePath, detector, stepscanMotor=G2_TRX, mvsampleMotor=
21 SAM_TRX, rotsampleMotor=SAM_ROT_Y, source_sample_d=None, sample_dect_d=None,
22 vertcenter=None):
23         self.stepscanMotor = stepscanMotor
24         self.rotsampleMotor = rotsampleMotor
25         self.mvsampleMotor = mvsampleMotor
26         self.source_sample_d = source_sample_d
27         self.sample_dect_d = sample_dect_d
28         self.vertcenter = vertcenter
29         if detector == 'Eiger':
30             self.detector = dect.Eiger(storagePath=storagePath, init=True)
31         elif detector == 'CdTe':
32             self.detector = dect.CdTe(storagePath=storagePath)
33         elif detector == 'PhotonicScience':
34             self.detector = dect.PhotonicScience(storagePath=storagePath)
35         # add different detectors here
36         else:
37             print("no such detector")
38
39     def sys_check(self, sample_in, sample_out):
40         """Perform system check."""
41         input("Check the detector parameters and press y (yes) to continue...")
42
43         self.rotsampleMotor.put(90, wait=True)
44         input("Check movement of sample rotation motor and press y (yes) to continue
45 ...")
46         self.rotsampleMotor.put(0, wait=True)
47
48         self.mvsampleMotor.mv(sample_out)
49         input("Check if sample out of the beam and press y (yes) to continue...")
50         self.mvsampleMotor.mv(sample_in)
```

```

48
49     self.stepscanMotor.mvr(6000)
50     input("Check if stepscan motor moved and press y (yes) to continue...")
51     self.stepscanMotor.mvr(-6000)
52
53     y = input("Check if x-rays are on and press y (yes) to continue")
54     print(y)
55
56     return y
57
58 def create_logfile(self, threshold, no_proj, angles_start, angles_end, expTime):
59     """Create a log file for a tomography."""
60     f = open(self.detector.storagePath + "logfile.txt", "a+")
61     f.write("Threshold: " + str(threshold) + "\n")
62     f.write("Exposure Time: " + str(expTime) + "\n")
63     f.write("Start Angle: " + str(angles_start) + "\n")
64     f.write("End Angle: " + str(angles_end) + "\n")
65     f.write("Number of Projections: " + str(no_proj) + "\n")
66     if self.source_sample_d is None:
67         source_sample_d = input("Source-sample distance for this setup has not
yet been entered. Enter source-to-sample distance in mm:")
68         self.source_sample_d = source_sample_d
69         f.write("Source to Sample (rotaxis): " + str(self.source_sample_d) + "mm" +
"\n")
70
71     if self.sample_dect_d is None:
72         sample_dect_d = input("Enter origin-to-detector distance in mm:")
73         self.sample_dect_d = sample_dect_d
74         f.write("Sample (rotaxis) to Detector: " + str(self.sample_dect_d) + "mm" +
"\n")
75
76     f.close()
77
78
79 def absorp_tomo(self, storagePath, threshold, sample_in, sample_out,
angles_degrees, expTime, source_sample_d=None, sample_dect_d=None, waitTime=None
, sys_check=True):
80     """Perform pure absorption tomography.
81
82     Parameters:
83     storagePath (str): wheret to save tomography
84     threshold (str): set detector threshold
85     sample_in (int): motor position when sample in the beam
86     sample_out (int): motor position when sample out of beam
87     angles_degrees (numpy array): angles where projections should be taken
88     expTime (int): exposure time for the projections in seconds
89     waitTime (int): default None, possible wait time for tube to warm up
90     """
91     self.detector.reinitialize()
92     self.detector.config_imgParams(nimages_per_file=5, ntrigger=100, nimages=1)
93     self.detector.config_storage_path(storagePath)
94     self.detector.config_energy(self.detector.photonEnergy, threshold)
95     self.detector.delete()
96

```

## B. Operation & Reconstruction Software

---

```
97     if sys_check:
98         y = self.sys_check(sample_in, sample_out)
99         if y is not 'y':
100             print("Exiting tomography...")
101             return
102
103     self.create_logfile(threshold, angles_degrees.shape[0], angles_degrees[0],
104                        angles_degrees[-1], expTime)
105
106     if waitTime is not None:
107         time.sleep(waitTime)
108
109     time1 = time.time()
110
111     self.rotsampleMotor.put(0, wait=True)
112
113     # flatfield
114     self.detector.config_imgParams(nimages_per_file=1, ntrigger=1, nimages=1)
115     self.mvsampleMotor.mv(sample_out)
116     self.detector.snap_one(expTime)
117
118     # tomography
119     self.detector.config_imgParams(nimages_per_file=5, ntrigger=100, nimages=1)
120     self.mvsampleMotor.mv(sample_in)
121
122     for i, angle in enumerate(angles_degrees):
123         print("Scanning at angle: ", angle)
124         self.rotsampleMotor.put(angle, wait=True)
125
126         if i%100 == 0:
127             self.detector.arm(expTime)
128             print("at image ", i, ", newly armed")
129
130             self.detector.trigger()
131
132         if i%100 == 99 or i == len(angles_degrees)-1:
133             self.detector.disarm()
134             print("at image ", i, ", newly disarmed")
135             self.detector.save()
136             self.detector.delete()
137
138     self.rotsampleMotor.put(0, wait=True)
139
140     # flatfield
141     self.detector.config_imgParams(nimages_per_file=1, ntrigger=1, nimages=1)
142     self.mvsampleMotor.mv(sample_out)
143     self.detector.snap_one(expTime)
144
145     self.mvsampleMotor.mv(sample_in)
146
147     time2 = time.time()
148     timetot = time2 - time1
149     print("Scan took ", timetot/60, " minutes")
```

```

150     f = open(self.detector.storagePath + "logfile.txt", "a+")
151     f.write("Acquisition Time: " + str(timetot) + "\n")
152     f.close()
153
154     def stepscan_tomo(self, storagePath, threshold, sample_in, sample_out,
155         angles_degrees, expTime, stepsize, source_sample_d=None, sample_dect_d=None,
156         waitTime=None, sys_check=True):
157         """Perform stepscan tomography.
158
159         Parameters:
160         storagePath (str): where to save tomography
161         threshold (str): set detector threshold
162         sample_in (int): motor position when sample in the beam
163         sample_out (int): motor position when sample out of beam
164         angles_degrees (numpy array): angles where projections should be taken
165         expTime (int): exposure time for the projections in seconds
166         stepsize (float): step size in um
167         waitTime (int): default None, possible wait time for tube to warm up
168         sys_check (bool): default True; lead through system inspection
169         """
170         self.detector.reinitialize()
171         self.detector.config_imgParams(nimages_per_file=5, ntrigger=100, nimages=1)
172         self.detector.config_storage_path(storagePath)
173         self.detector.config_energy(self.detector.photonEnergy, threshold)
174         self.detector.delete()
175
176         if sys_check:
177             y = self.sys_check(sample_in, sample_out)
178             if y is not 'y':
179                 print("Exiting tomography...")
180                 return
181
182             self.create_logfile(threshold, angles_degrees.shape[0], angles_degrees[0],
183             angles_degrees[-1], expTime)
184
185             if waitTime is not None:
186                 time.sleep(waitTime)
187
188             time1 = time.time()
189
190             self.rotsampleMotor.put(0, wait=True)
191
192             # flatfield
193             self.detector.config_imgParams(nimages_per_file=5, ntrigger=5, nimages=1)
194             self.mvsampleMotor.mv(sample_out)
195             self.step_scan(5, stepsize, expTime)
196
197             # tomography
198             self.detector.config_imgParams(nimages_per_file=5, ntrigger=100, nimages=1)
199             self.mvsampleMotor.mv(sample_in)
200
201             for i, angle in enumerate(angles_degrees):
202                 print("Scanning at angle: ", angle)
203                 self.rotsampleMotor.put(angle, wait=True)

```

## B. Operation & Reconstruction Software

---

```
201
202     if i%20 == 0:
203         self.detector.arm(expTime)
204         print("at image ", i, ", newly armed")
205
206     self.step_scan(5, stepsize, expTime, saving=False)
207
208     if i%20 == 19 or i == len(angles_degrees)-1:
209         self.detector.disarm()
210         print("at image ", i, ", newly disarmed")
211         self.detector.save()
212         self.detector.delete()
213
214     self.rotsampleMotor.put(0, wait=True)
215
216     # flatfield
217     self.detector.config_imgParams(nimages_per_file=5, ntrigger=5, nimages=1)
218     self.mvsampleMotor.mv(sample_out)
219     self.step_scan(5, stepsize, expTime)
220
221     self.mvsampleMotor.mv(sample_in)
222
223     time2 = time.time()
224     timetot = time2 - time1
225     print("Scan took ", timetot/60, " minutes")
226
227     f = open(self.detector.storagePath + "logfile.txt", "a+")
228     f.write("Acquisition Time: " + str(timetot) + "\n")
229     f.close()
230
231 def step_scan(self, n_steps, step, expTime, saving=True, storagePath=None):
232     """Perform a single step scan.
233
234     Parameters:
235     n_steps (int): number of steps over one period
236     step (float): the step size in um
237     expTime (int): exposure time of single image
238     saving (bool): saves step scan by default to the detector storage path
239     storagePath (str): default is detector storage path
240     """
241     self.detector.config_imgParams(nimages_per_file=n_steps, ntrigger=n_steps,
nimages=1)
242     init_pos = self.stepscanMotor.get_position()
243     if storagePath is not None:
244         old_path = self.detector.storagePath
245         self.detector.config_storage_path(storagePath)
246
247     if saving:
248         print("Scan will be saved to: " + self.detector.storagePath)
249         self.detector.arm(expTime)
250     for i in range(n_steps):
251         self.detector.trigger()
252         self.stepscanMotor.mvr(step)
253     if saving:
```

```

254         self.detector.disarm()
255         self.detector.save()
256         self.detector.delete()
257     self.stepscanMotor.mv(init_pos)
258
259     # reset defaults
260     self.detector.config_imgParams(nimages_per_file=5, ntrigger=100, nimages=1)
261     if storagePath is not None:
262         self.detector.config_storage_path(old_path)
263
264     # these two functions are so far only experimental, they have not been tested
    yet
265     def take_ff(self, before_position):
266         self.rotsampleMotor.put(0, wait=True)
267         self.detector.config_imgParams(nimages_per_file=5, ntrigger=5, nimages=1)
268         self.mvsampleMotor.mv(sample_out)
269         self.step_scan(5, stepsize, expTime)
270         self.mvsampleMotor.mv(sample_in)
271         self.rotsampleMotor.put(before_position, wait=True)
272
273     def stepscan_tomo_flatfield(self, storagePath, threshold, sample_in, sample_out,
    angles_degrees, expTime, stepsize, source_sample_d=None, sample_dect_d=None,
    waitTime=None, sys_check=True):
274         self.detector.reinitialize()
275         self.detector.config_imgParams(nimages_per_file=5, ntrigger=100, nimages=1)
276         self.detector.config_storage_path(storagePath)
277         self.detector.config_energy(self.detector.photonEnergy, threshold)
278         self.detector.delete()
279
280         if sys_check:
281             y = self.sys_check(sample_in, sample_out)
282             if y is not 'y':
283                 print("Exiting tomography...")
284                 return
285
286         self.create_logfile(threshold, angles_degrees.shape[0], angles_degrees[0],
    angles_degrees[-1], expTime)
287
288         if waitTime is not None:
289             time.sleep(waitTime)
290
291         time1 = time.time()
292
293         self.rotsampleMotor.put(0, wait=True)
294
295         # initial flatfield
296         self.take_ff(0)
297
298         # tomography settings
299         self.detector.config_imgParams(nimages_per_file=5, ntrigger=100, nimages=1)
300         self.mvsampleMotor.mv(sample_in)
301
302         for i, angle in enumerate(angles_degrees):
303             print("Scanning at angle: ", angle)

```

## B. Operation & Reconstruction Software

---

```
304         self.rotsampleMotor.put(angle, wait=True)
305
306         if i%20 == 0:
307             self.detector.arm(expTime)
308             print("at image ", i, ", newly armed")
309
310         self.step_scan(5, stepsize, expTime, saving=False)
311
312         if i%20 == 19 or i == len(angles_degrees)-1:
313             self.detector.disarm()
314             print("at image ", i, ", newly disarmed")
315             self.detector.save()
316             self.detector.delete()
317             self.take_ff(angle)
318
319         time2 = time.time()
320         timetot = time2 - time1
321         print("Scan took ", timetot/60, " minutes")
322
323         f = open(self.detector.storagePath + "logfile.txt", "a+")
324         f.write("Acquisition Time: " + str(timetot) + "\n")
325         f.close()
326
327         # this remains here for the moment in order to keep old notebooks working
328         # in principle you don't need it anymore
329         def fba(self, data, periods=0):
330             """Implementation of fba function."""
331             data = np.transpose(data, axes=(1,2,0))
332             fdata = npfft.fft(data)
333             A = np.abs(fdata[:, :, 0])
334             B = np.abs(fdata[:, :, periods+1])
335             P = np.angle(fdata[:, :, periods+1])
336             return (A, B, P)
```

## B.4. Data Processing Software

List. B.3: data\_processing.py

```
1  import time
2  import numpy as np
3  import numpy.fft as npfft
4  import matplotlib.pyplot as plt
5  import os
6  import sys
7  import glob
8  import h5py
9  import hdf5plugin
10 from scipy.signal import argrelextrema
11 import re
12
```

```

13 def plot_vismap(vis):
14     """Plot visibility map of the scan.
15
16     Parameters:
17     vis (2D/3D nparray): visibility from a scan or the scan itself
18     """
19     if vis.ndim is 3:
20         vis = visibility(vis)
21     plt.figure(figsize=(10, 10))
22     plt.colorbar(plt.imshow(vis, cmap='gray'))
23     plt.title("Visibility Map")
24     plt.show()
25
26 def plot_phasemap(phase):
27     """Plot phase of the scan.
28
29     Parameters:
30     phase (2D/3D nparray): Pref from a scan or the scan itself
31     """
32     if phase.ndim is 3:
33         a0, a1, phase = fba(phase)
34     plt.figure(figsize=(10, 10))
35     plt.colorbar(plt.imshow(phase, cmap='gray', vmin = -3.14, vmax = 3.14))
36     plt.title("Phase Map")
37     plt.show()
38
39 def plot_vishistogram(vis, peak=True):
40     """Plot the visibility histogram.
41
42     Parameters:
43     vis (2D nparray): visibility of a scan
44     peak (bool): plot the peak value
45     """
46     if vis.ndim == 3:
47         vis = visibility(vis)
48
49     if peak is True:
50         height, visib = np.histogram(vis[vis<1], range=(0,0.3), bins=256)
51         a = argrelextrema(height, comparator=np.greater, order=1000)
52         peak_val = visib[a[0][0]]
53
54     plt.hist(vis[vis<1], bins = 256, range=(0,0.4))
55
56     if peak is True:
57         plt.title("Visibility Histogram, peak: " + str(peak_val)[:5])
58     elif peak is False:
59         plt.title("Visibility Histogram")
60
61     plt.show()
62
63 def visibility(flatfield):
64     """Calculate visibility of 3D phase step set.
65
66     Parameters:

```

## B. Operation & Reconstruction Software

---

```
67     flatfield (3D nparray): stepscan data
68
69     Return:
70     visibility (2D nparray): visibility distribution
71     """
72     A0, A1, P1 = fba(flatfield)
73     return 2*A1/A0
74
75 def angular_sensitivity(period, G1_G2, diff_phase, source_G1=1, source_sam=1):
76     """Return angular sensitivity from diff phase image.
77
78     For short setups: definitely make use of last two arguments
79
80     Parameters:
81     period (float): grating period in m
82     G1_G2 (int): propagation distance in m
83     diff_phase (2D np.array): area of diff phase image that should be looked at
84     source_G1 (int): distance source-G1
85     source_sam (int): distance source-sample
86     """
87     return period*source_G1 / (2*np.pi*G1_G2*source_sam) * np.std(diff_phase)
88
89 def fba(data):
90     """Return Fourier coefficients.
91
92     Parameters:
93     data (3D nparray): stepscan data
94
95     Return:
96     (A0, A1, P1): Fourier coeff and phase needed for visibility and imaging
97     """
98     fdata = npfft.fft(data, axis=0)
99     A0 = np.abs(fdata[0])
100    A1 = np.abs(fdata[1])
101    P1 = np.angle(fdata[1])
102    return (A0, A1, P1)
103
104 def show(image, ROI=np.s_[ :,:], vmin=None, vmax=None, figsize=(10, 10)):
105     """Show an image.
106
107     Parameters:
108     image (numpy.array): 2D or 3D numpy array containing the image to be shown, 0
109     will be shown for 3D
110     ROI (numpy.s_): 2D numpy slice for zooming into specific region
111     vmin (float): min data range
112     vmax (float): max data range
113     figsize (float, float): float tuple, size in inches (fuck imperial!)
114     """
115     if image.ndim is 3:
116         image = image[0]
117     plt.subplots(figsize=figsize)
118     plt.imshow(image[ROI], cmap='gray', vmin=vmin, vmax=vmax)
119
120 def show_parallel(images, ROI=np.s_[ :,:], vmin=None, vmax=None, figsize=(15,15)):
```

```

120     """Show several images next to each other
121
122     Parameters:
123     image (numpy.array or list): 3D numpy array or list of 2D numpy arrays
124     containing images to be shown
125     ROI (numpy.s_): 2D numpy slice for zooming into specific region
126     vmin (float): min data range
127     vmax (float): max data range
128     figsize (float, float): float tuple, size in inches (fuck imperial!)
129     """
130     if type(images) is list:
131         no_plots = len(images)
132     else:
133         no_plots = images.shape[0]
134     fig, axs = plt.subplots(1, no_plots, figsize=figsize)
135     for i in range(no_plots):
136         axs[i].imshow(images[i][ROI], cmap='gray', vmin=vmin, vmax=vmax)
137     plt.show()
138
139 def remove_nans(data):
140     """Set all NaN's from a dataset to 0."""
141
142     nans = np.isnan(data)
143     data[nans] = 0
144     return data
145
146 def make_sino(data):
147     """Make sinograms from projection data."""
148
149     return np.transpose(data, axes=(1,0,2))
150
151 def extract_3_images(data, ff, amp=False, dpc=False, dci=False):
152     """Convert dataset into absorption, differential phase contrast and dark field
153     images.
154
155     Currently uses only the first flatfield.
156
157     Parameters:
158     data (4D numpy array, 3D if single_step): contains phase steps of projections
159         in case of 4D: 0 dimension - for different projections
160         1 dimension - same projection, step scan
161         2,3 - image itself
162     in case of 3D: same as above for 1-3
163     ff (4D numpy array, 3D if single_step): contains flatfield phase steps
164     amp (bool): default True
165     dpc (bool): default True
166     dci (bool): default True
167
168     Return:
169     imgs (tuple): 3D numpy arrays containing the three respective sets of
170     projections
171     """
172     if data.ndim is 3:

```

## B. Operation & Reconstruction Software

---

```
171     A0ref, A1ref, P1ref = fba(ff)
172     A0sam, A1sam, P1sam = fba(data)
173
174     amp_arr = -np.log(A0sam/A0ref)
175     dpc_arr = np.angle(np.exp(1j*(P1sam-P1ref)))
176     dci_arr = -np.log(A1sam/A1ref*A0ref/A0sam)
177
178     return amp_arr, dpc_arr, dci_arr
179
180     if amp:
181         amp_arr = np.zeros((data.shape[0], data.shape[2], data.shape[3]))
182     if dpc:
183         dpc_arr = np.zeros((data.shape[0], data.shape[2], data.shape[3]))
184     if dci:
185         dci_arr = np.zeros((data.shape[0], data.shape[2], data.shape[3]))
186
187     # flatfield iteration to be implemented
188     A0ref, A1ref, P1ref = fba(ff[0]) # currently only using the first flatfield
189
190     for i in np.arange(data.shape[0]):
191         A0sam, A1sam, P1sam = fba(data[i])
192
193         if amp:
194             amp_arr[i] = -np.log(A0sam/A0ref)
195         if dpc:
196             dpc_arr[i] = np.angle(np.exp(1j*(P1sam-P1ref)))
197         if dci:
198             dci_arr[i] = -np.log(A1sam/A1ref*A0ref/A0sam)
199
200     imgs = []
201     if amp:
202         imgs.append(amp_arr)
203     if dpc:
204         imgs.append(dpc_arr)
205     if dci:
206         imgs.append(dci_arr)
207
208     if len(imgs) is 1:
209         return imgs[0]
210
211     return tuple(imgs)
212
213
214 def get_masterlist(folder, master_max=None):
215     """Create a list of masterfiles from folder. (EIGER ONLY)
216
217     Parameters:
218     folder (str): path to folder with masterfiles
219     master_max (int): seqID of last file
220
221     Returns:
222     masters (list of str): list containing paths to masterfiles
223     """
224     if master_max is not None:
```

```

225     masters = [None]*master_max
226     for i in range(1, master_max+1):
227         masters[i-1] = get_masterfile(folder, i)
228     else:
229         contains_master = lambda x: ("_master") in x
230         path = os.path.join(folder, '')
231         files = list(filter(os.path.isfile and contains_master, glob.glob(path + '**
232     )))
232     masters = sorted(files, key = lambda x: int(re.findall(r'\d+', os.path.
233     splitext(os.path.basename(x))[0])[0]))
234     return masters
235
236 def get_masterfile(path, sequence_id):
237     """Return path to master file with specified sequence ID. (EIGER ONLY)
238
239     Parameters:
240     path (str): path to folder which contains masterfiles
241     sequence_id (int): which file to get path from
242
243     Returns:
244     file (str): path to masterfile
245     """
246     contains_id = lambda x: ("_" + str(sequence_id) + "_master") in x
247     path = os.path.join(path, '')
248     file = list(filter(os.path.isfile and contains_id, glob.glob(path + '**
249     )))
250     return file[0]
251
252 def master_3D(masters, no_proj, sino_slice=np.s_[:]):
253     """Create 3D array from list of masterfiles. (EIGER ONLY)
254
255     Parameters:
256     masters (list of str): list of paths to sorted masterfiles
257     no_proj (int): number of total projections
258     sino_slice (np.s_ object): specify which sinograms in vert direction to load
259
260     Returns:
261     data (3D numpy array): array containing projections
262     """
263     with h5py.File(masters[0], 'r') as f:
264         x = f['entry']['data']['data_000001'][()].shape[1]
265         y = f['entry']['data']['data_000001'][()].shape[2]
266
267     x = len(np.zeros(x)[sino_slice])
268     data = np.zeros((no_proj, x, y))
269
270     enumerator = 0
271
272     for master in masters:
273         with h5py.File(master, 'r') as f:
274             for datafile in list(f['entry']['data'].keys()):
275                 try:
276                     data[enumerator:enumerator+5] = f['entry']['data'][datafile][()]
277                 ][:][sino_slice]

```

```

276         enumerator += 5
277     except:
278         print("dangerous situation, check ", master, datafile)
279         break
280
281     return data
282
283 def master_4D(masters, no_of_projections, sino_slice=np.s_[:]):
284     """Create 4D array from list of masterfiles. (EIGER ONLY)
285
286     Parameters:
287     masters (list of str): list of paths to sorted masterfiles
288     no_proj (int): number of total projections
289     sino_slice (np.s_ object): specify which sinograms in vert direction to load
290
291     Returns:
292     data (4D numpy array): array containing phase steps of projections
293     """
294     mylist = []
295     for master in masters:
296         with h5py.File(master, 'r') as f:
297             for datafile in list(f['entry']['data'].keys()):
298                 try:
299                     mylist.append(f['entry']['data'][datafile][()][: , sino_slice])
300                 except:
301                     print("dangerous situation, check ", master, datafile)
302                     break
303     mylist = np.asarray(mylist)
304     if mylist.shape[0] == no_of_projections:
305         return mylist
306     else:
307         print("Check if everything has been added")
308         return mylist
309
310 def master_to_array(file):
311     """Return 3D numpy array of images stored in master file. (EIGER ONLY)
312
313     Parameters:
314     file (str): path to h5 master file containing images
315     onylfirst (bool): helpful if only one set of phase steps needed
316
317     Returns:
318     arr (3D numpy array): dataset from this file
319     """
320     arr = []
321     with h5py.File(file, 'r') as f:
322         for i in list(f['entry']['data'].keys()):
323             try:
324                 arr.append(f['entry']['data'][i][()])
325             except:
326                 print("Some images might not have been added due to corrupted file
327                 links")
327                 break
328     return np.asarray(arr)[0]

```

List. B.4: Reconstruction.py

```

1  import astra
2  import numpy as np
3
4  class Reconstruction:
5      def __init__(self, geometry, algorithm, rotcenter, angles, source_origin,
6                  origin_detector, pixel_size, data, filtertype=None, vertcenter=None,
7                  phase_contrast=False):
8          """Create new instance of Tomographic Reconstruction.
9
10         Parameters:
11         geometry (str): 'fanflat' or 'cone'
12         algorithm (str): 'SIRT3D_CUDA', 'FDK_CUDA' for cone; 'FBP_CUDA', 'SIRT_CUDA'
13         for fanflat; see astra-toolbox.com
14         rotcenter (float): pixel specifying rotation center from left side of
15         projection
16         angles (numpy array): listing the projection angles in radians
17         source_origin (float): distance in mm
18         origin_detector (float): distance in mm
19         pixel_size (float): size in mm
20         data (3D numpy array): sinogram data
21         filtertype (str): default 'ram-lak', check astra-toolbox.com
22         vertcenter (float): pixel specifying center of cone beam from top (IMPORTANT
23         : center sino must be part of dataset)
24         phase_contrast (bool): default False, set True if reconstructing DPC images
25         """
26         self.geometry = geometry
27         self.algorithm = algorithm
28         self.rotcenter = rotcenter
29         self.vertcenter = vertcenter
30         self.angles = angles
31         self.source_origin = source_origin
32         self.origin_detector = origin_detector
33         self.pixel_size = pixel_size
34         self.data = data
35         self.detector_rows = self.data.shape[0]
36         self.detector_cols = self.data.shape[2]
37         self.filtertype = filtertype
38
39         sino_center = self.data.shape[2] / 2
40         off_center = sino_center - self.rotcenter
41
42         if vertcenter is not None:
43             proj_center = self.data.shape[0] / 2
44             vert_offcenter = proj_center - self.vertcenter
45
46         # implement 2D geometries here
47         if self.geometry is 'fanflat':
48             self.algos = []
49             for sino in np.arange(self.data.shape[0]):
50                 proj_geom = astra.create_proj_geom(self.geometry, 1, self.

```

```

    detector_cols, self.angles, (self.source_origin + self.origin_detector) / self.
    pixel_size, 0)
46     proj_geom = astra.functions.geom_postalignment(proj_geom, off_center
    )
47
48     vol_geom = astra.creators.create_vol_geom(self.detector_cols)
49
50     projections_id = astra.data2d.create('-sino', proj_geom, self.data[
    sino])
51
52     reconstruction_id = astra.data2d.create('-vol', vol_geom, data=0)
53
54     alg_cfg = astra.astra_dict(self.algorithm)
55     alg_cfg['ProjectionDataId'] = projections_id
56     alg_cfg['ReconstructionDataId'] = reconstruction_id
57     if self.algorithm is 'FBP_CUDA':
58         alg_cfg['option'] = {'FilterType': self.filtertype}
59
60     if self.algorithm is 'SIRT_CUDA':
61         alg_cfg['option'] = {'MinConstraint': 0}
62
63     if phase_contrast:
64         alg_cfg['option'] = {'FilterType': 'Hilbert'}
65
66     algorithm_id = astra.algorithm.create(alg_cfg)
67
68     self.algos.append([proj_geom, vol_geom, projections_id,
    reconstruction_id, algorithm_id])
69
70     # implement 3D geometries here
71     if self.geometry is 'cone':
72         self.proj_geom = astra.create_proj_geom('cone', 1, 1, self.detector_rows
    , self.detector_cols, self.angles, (self.source_origin + self.origin_detector) /
    self.pixel_size, 0)
73         self.proj_geom = astra.functions.geom_postalignment(self.proj_geom, [
    off_center, vert_offcenter])
74
75         self.projections_id = astra.data3d.create('-sino', self.proj_geom, self.
    data)
76
77         self.vol_geom = astra.creators.create_vol_geom(self.detector_cols, self.
    detector_cols, self.detector_rows)
78
79         self.reconstruction_id = astra.data3d.create('-vol', self.vol_geom, data
    =0)
80
81         self.alg_cfg = astra.astra_dict(self.algorithm)
82         self.alg_cfg['ProjectionDataId'] = self.projections_id
83         self.alg_cfg['ReconstructionDataId'] = self.reconstruction_id
84         if self.algorithm is 'FDK_CUDA':
85             self.alg_cfg['option'] = {'FilterType': self.filtertype}
86
87         if self.algorithm is 'SIRT3D_CUDA':
88             self.alg_cfg['option'] = {'MinConstraint': 0}

```

```

89
90     if phase_contrast:
91         self.alg_cfg['option'] = {'FilterType': 'Hilbert'}
92
93         self.algorithm_id = astra.algorithm.create(self.alg_cfg)
94
95 def run(self, iterations=None):
96     """Run the created algorithm. Specify number of iterations for SIRT"""
97
98     if self.algorithm is 'SIRT3D_CUDA':
99         astra.algorithm.run(self.algorithm_id, iterations)
100        recon = astra.data3d.get(self.reconstruction_id)
101    elif self.algorithm is 'FDK_CUDA' or self.algorithm is 'BP3D_CUDA':
102        astra.algorithm.run(self.algorithm_id)
103        recon = astra.data3d.get(self.reconstruction_id)
104    else:
105        recon = []
106        for sino in self.algos:
107            proj_geom = sino[0]
108            vol_geom = sino[1]
109            projections_id = sino[2]
110            reconstruction_id = sino[3]
111            algorithm_id = sino[4]
112            if self.algorithm is 'SIRT_CUDA':
113                astra.algorithm.run(algorithm_id, iterations)
114            else:
115                astra.algorithm.run(algorithm_id)
116                recon.append(astra.data2d.get(reconstruction_id))
117        recon = np.asarray(recon)
118    return recon
119
120 def project_phantom(angles, source_origin, origin_detector, pixel_size, phantom,
121                    rotcenter=None, vertcenter=None):
122     """Create a set of projections using a cone beam shaped projector"""
123
124     det_rows = phantom.shape[0]
125     det_cols = phantom.shape[1]
126
127     if rotcenter is not None:
128         sino_center = phantom.shape[1] / 2
129         off_center = sino_center - rotcenter
130     else:
131         off_center = 0
132
133     if vertcenter is not None:
134         proj_center = phantom.shape[0] / 2
135         vert_offcenter = proj_center - vertcenter
136     else:
137         vert_offcenter = 0
138
139     vol_geom = astra.creators.create_vol_geom(det_cols, det_cols, det_rows)
140
141     phantom_id = astra.data3d.create('-vol', vol_geom, data=phantom)

```

## B. Operation & Reconstruction Software

---

```
142
143     proj_geom = astra.create_proj_geom('cone', 1, 1, det_rows, det_rows, angles, (
144     source_origin + origin_detector) / pixel_size, 0)
145     proj_geom = astra.functions.geom_postalignment(proj_geom, [off_center,
146     vert_offcenter])
147
148     projections_id, projections = astra.creators.create_sino3d_gpu(phantom_id,
149     proj_geom, vol_geom)
150
151     projections = np.transpose(projections, axes=(1, 0, 2))
152     return projections
```

## REFERENCES

- [1] University of Calgary, ed. *CT Image Reconstruction*. URL: [http://199.116.233.101/index.php?title=CT\\_Image\\_Reconstruction#Sinogram\\_and\\_Radon\\_transform](http://199.116.233.101/index.php?title=CT_Image_Reconstruction#Sinogram_and_Radon_transform) (visited on 05/22/2021).
- [2] William B. Case et al. “Realization of optical carpets in the Talbot and Talbot-Lau configurations”. In: *Opt. Express* 17.23 (Nov. 2009), pp. 20966–20974. DOI: 10.1364/OE.17.020966. URL: <http://www.opticsexpress.org/abstract.cfm?URI=oe-17-23-20966>.
- [3] Tilman Donath et al. “Inverse geometry for grating-based x-ray phase-contrast imaging”. In: *Journal of Applied Physics* 106 (Oct. 2009), pp. 054703–054703. DOI: 10.1063/1.3208052.
- [4] M Engelhardt et al. “The fractional Talbot effect in differential x-ray phase-contrast imaging for extended and polychromatic x-ray sources”. In: *Journal of microscopy* 232 (Nov. 2008), pp. 145–57. DOI: 10.1111/j.1365-2818.2008.02072.x.
- [5] Aaron Filler. “The History, Development and Impact of Computed Imaging in Neurological Diagnosis and Neurosurgery: CT, MRI, and DTI”. In: *Internet Journal of Neurosurgery* 7 (May 2010), pp. 1–85. DOI: 10.1038/npre.2009.3267.5.
- [6] Gabor T. Herman. *Fundamentals of Computerized Tomography, Image Reconstruction from Projections*. Second Edition. Springer-Verlag London Limited, 2009.
- [7] Gabor T. Herman. *Fundamentals of Computerized Tomography, Image Reconstruction from Projections*. 2009.
- [8] Dectris Ltd., ed. *EIGER2 R for Laboratory*. URL: <https://www.dectris.com/products/eiger2/eiger2-r-for-laboratory/> (visited on 05/19/2021).
- [9] Dectris Ltd., ed. *User Manual Eiger R/X Detector Systems*. URL: [https://media.dectris.com/UserManual\\_EIGER.pdf](https://media.dectris.com/UserManual_EIGER.pdf) (visited on 05/05/2021).
- [10] Daniël M. Pelt et al. “Integration of TomoPy and the ASTRA toolbox for advanced processing and reconstruction of tomographic synchrotron data”. In: *Journal of Synchrotron Radiation* 23.3 (May 2016), pp. 842–849. DOI: 10.1107/S1600577516005658. URL: <https://doi.org/10.1107/S1600577516005658>.

- [11] Franz Pfeiffer et al. “Phase retrieval and differential phase-contrast imaging with low-brilliance X-ray sources”. In: *Nature Physics* 2.4 (Apr. 2006), pp. 258–261. ISSN: 1745-2481. DOI: 10.1038/nphys265. URL: <https://doi.org/10.1038/nphys265>.
- [12] Lord Rayleigh. *The London, Edinburgh and Dublin Philosophical Magazine and Journal of Science*. XXV. On Copying Diffraction-gratings, and some Phenomena connected therewith. Taylor & Francis, 1881. URL: <https://books.google.ch/books?id=05E0AAAAIAAJ>.
- [13] Tom Roelandts, ed. *Tomography, Part 3: Reconstruction*. URL: <https://tomroelandts.com/articles/tomography-part-3-reconstruction> (visited on 05/18/2021).
- [14] Tom Roelandts, ed. *Tomography, Part 3: Reconstruction*. URL: <https://tomroelandts.com/articles/tomography-part-3-reconstruction> (visited on 05/18/2021).
- [15] A. Snigirev et al. “On the possibilities of x-ray phase contrast microimaging by coherent high-energy synchrotron radiation”. In: *Review of Scientific Instruments* 66.12 (1995), pp. 5486–5492. DOI: 10.1063/1.1146073. eprint: <https://doi.org/10.1063/1.1146073>. URL: <https://doi.org/10.1063/1.1146073>.
- [16] Thomas J. Suleski. “Generation of Lohmann images from binary-phase Talbot array illuminators”. In: *Appl. Opt.* 36.20 (July 1997), pp. 4686–4691. DOI: 10.1364/AO.36.004686. URL: <http://ao.osa.org/abstract.cfm?URI=ao-36-20-4686>.
- [17] T. Thuering and M. Stampanoni. “Performance and optimization of X-ray grating interferometry”. In: *Philosophical Transactions of the Royal Society A: Mathematical, Physical and Engineering Sciences* 372.2010 (2014), p. 20130027. DOI: 10.1098/rsta.2013.0027. eprint: <https://royalsocietypublishing.org/doi/pdf/10.1098/rsta.2013.0027>. URL: <https://royalsocietypublishing.org/doi/abs/10.1098/rsta.2013.0027>.
- [18] Thomas Thuering et al. “Sensitivity in X-ray grating interferometry on compact systems”. In: *AIP Conference Proceedings* 1466.1 (2012), pp. 293–298. DOI: 10.1063/1.4742307. eprint: <https://aip.scitation.org/doi/pdf/10.1063/1.4742307>. URL: <https://aip.scitation.org/doi/abs/10.1063/1.4742307>.
- [19] Thomas Thüring. “Compact X-ray grating interferometry for phase and dark-field computed tomography in the diagnostic energy range”. en. PhD thesis. Zürich: ETH Zurich, 2013. DOI: 10.3929/ethz-a-010008147.
- [20] Mathias Tomandl. “Realisierung von optischen Talbot- und Talbot-Lau-Teppichen”. PhD thesis. 2013. URL: [http://othes.univie.ac.at/9413/1/2010-04-22\\_0402570.pdf](http://othes.univie.ac.at/9413/1/2010-04-22_0402570.pdf).

- [21] Joan Vila-Comamala et al. “High sensitivity X-ray phase contrast imaging by laboratory grating-based interferometry at high Talbot order geometry”. In: *Opt. Express* 29.2 (Jan. 2021), pp. 2049–2064. DOI: 10.1364/OE.414174. URL: <http://www.opticsexpress.org/abstract.cfm?URI=oe-29-2-2049>.
- [22] Timm Weitkamp et al. “Tomography with grating interferometers at low-brilliance sources”. In: *Developments in X-Ray Tomography V*. Ed. by Ulrich Bonse. Vol. 6318. International Society for Optics and Photonics. SPIE, 2006, pp. 249–258. DOI: 10.1117/12.683851. URL: <https://doi.org/10.1117/12.683851>.
- [23] Timm Weitkamp et al. “X-ray phase imaging with a grating interferometer”. In: *Opt. Express* 13.16 (Aug. 2005), pp. 6296–6304. DOI: 10.1364/OPEX.13.006296. URL: <http://www.opticsexpress.org/abstract.cfm?URI=oe-13-16-6296>.



## IMAGE SOURCES

- [1] University of Calgary, ed. *CT Image Reconstruction*. URL: [http://199.116.233.101/index.php?title=CT\\_Image\\_Reconstruction#Sinogram\\_and\\_Radon\\_transform](http://199.116.233.101/index.php?title=CT_Image_Reconstruction#Sinogram_and_Radon_transform) (visited on 05/22/2021).
- [7] Gabor T. Herman. *Fundamentals of Computerized Tomography, Image Reconstruction from Projections*. 2009.
- [13] Tom Roelandts, ed. *Tomography, Part 3: Reconstruction*. URL: <https://tomroelandts.com/articles/tomography-part-3-reconstruction> (visited on 05/18/2021).